

INTERUNIS-IT

A-Line

User manual supplement

2024



WARNING! Changes may have been made to the software that are not reflected in this manual.

The settings shown in the figures are used as examples. Real values should be chosen based on specific conditions.

Table of Contents

Table of Contents	3
Chapter 1. Short description	5
Section 1. A-Line	6
Chapter 2. Using location areas	7
2.1. Description of how it works	7
2.2. Application example	7
Chapter 3. Application of the informational statistical AE criterion	14
3.1. Description of how it works	14
3.2. Application examples	18
3.3. Conclusions	23
3.4. References	23
Chapter 4. Arbitrary antenna fuzzy locating (AAFL)	24
4.1. Differences between the AAFL method and location with triangular and quadrangular antennas (LA3 and LA4)	24
4.2. Short explanation of the AAFL method	25
4.3. A quick guide to using the AAFL method	26
An accurate description of the object's geometric shape	26
Channel settings	26
Selection of velocity range	27
Setting the lattice parameters	28
Setting pack options	29
Configuring clustering options	30
4.4. AAFL example	30
Chapter 5. Calibration procedure	36
5.1. Channel calibration	36
Used abbreviations and terms	36
Calibration overview	36
General settings	37
Setting up a noise level test	40
Setting up a calibration test	44
Settings and calibration algorithm	46
Running tests and calibrations	50

Section 2. A-Line OSC	53
Chapter 6. Wavelet analysis of AE impulses in thin-walled objects	
6.1. Guided waves	54
6.2. Wavelet transform	56
6.3. Little help for beginners	60
6.4. References	61
Chapter 7. Manufacturer information	64



Chapter 1. Short description

Many years of experience of INTERUNIS-IT in the field of non-destructive testing has made it possible to create a family of **A-Line** digital hardware and software systems designed for multichannel registration and measurement of parameters of acoustic emission electrical signals in order to evaluate the technical condition of hazardous production facilities during non-destructive testing.

This manual applies to software of acoustic emission measuring systems **A-Line PCI**, **A-Line DDM**, **A-Line DS** (hereinafter referred to as **A-Line** complexes), which are multichannel measuring automated complexes for receiving and processing information from the testing object in the process of acoustic emission testing. The phenomenon of acoustic emission (AE) consists in the emission of acoustic waves by an object under the influence of a loading or under the influence of other factors. Information is received from a variety of acoustic emission sensors, which receive acoustic waves propagating in the testing object and convert them into an AE electrical signal, which is then amplified by a built-in or external preamplifier, converted to digital form and processed in order to detect developing defects, their localization and determination of the degree of danger.

The **A-Line** complexes include one or more computer-based data acquisition and processing units, external devices connected to them and the **A-Line** software common for all complexes of the family. The **A-Line** software provides extensive control over data acquisition, processing and presentation of measurement results, both in real time and in post-processing mode. In addition to the main program, INTERUNIS-IT also created the program **A-Line OSC**, which allows for more detailed processing of waveforms, and the program **A-Line Stat**, designed for statistical processing of acoustic emission data.



Recording of waveforms is carried out by the main program **A-Line**, and subsequent processing can be performed both by the main program **A-Line** and additional programs **A-Line OSC** and **A-Line Stat**.



Section 1

A-Line

Chapter 2. Using location areas



Chapter “*Using location areas*” provides an example of using location areas. The corresponding technique is built into the A-Line software of INTERUNIS-IT.

2.1. Description of how it works

The main idea of using location areas is as follows: according to the results of preliminary flaw detection or structural analysis, the testing object is divided into a certain finite number of elements (location areas), in the general case, unequal and heterogeneous, within which their properties can be considered the same and known, and the acoustic characteristics are quite favorable for reliable and reliable location of defects. Further, each of the received elements is assigned some individual critical number of located AE events, the excess of which, under certain conditions, will mean the beginning of significant changes in this place, requiring some kind of reaction or, at least, a special mode for displaying the results due to their importance at the stage of data acquisition.

Setting up location areas is described in the User manual in the chapter **Location areas**.

It is useful, for clarity, to overlay background images in *.emf format for the 2D type of drawing and three-dimensional models in the *.ase format for the 3D type on the final window for displaying the results of the work of the location areas from the command line when starting the program. A characteristic scope of application of location areas is the repeated testing of a large number of similar, well-studied objects in automatic or semi-automatic mode. In this case, having a sufficient knowledge base, it is possible to build an exhaustive system of multi-stage hazard criteria. It is also useful to use the combination of location areas and a parametric gate in location to achieve a higher level of reliability of the results.

2.2. Application example

Let's consider the use of location areas using the example of linear location.

An example containing files for the A-Line program of versions not lower than 4.91 can be downloaded from the site at: <http://interunis-it.ru/ru/info/downloads/>. Archive contains files:

- ◇ A.cfg is configuration settings file (windows and hardware settings);
- ◇ A.lfg is location settings file;
- ◇ A.emf is image file for displaying location areas;
- ◇ A.crg is location area settings file;
- ◇ A.bat is the batch file.

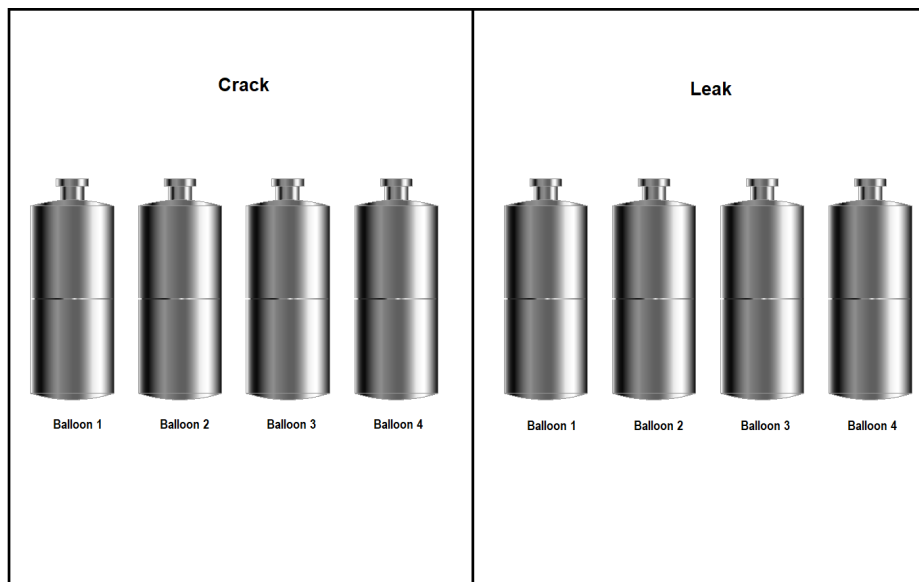


Fig. 2.1. A.emf is image file for displaying location areas

In an already running program, you need to carry out the following manipulations:

- ◇ Load A.cfg settings file. To do this, use the main menu **File – Open Config** to specify the path to the corresponding configuration file. Together with settings of windows displaying AE information, this file contains parametric input settings (coefficients K1 and K2 specify the linear conversion of current from the parametric input into pressure in kPa (Fig. 2.2)). In addition to these, the file contains information on two hardware profiles "Crack" and "Leak" (Fig. 2.3). The first profile is characterized by a fixed threshold, the second is characterized by a floating threshold with a value of 3 dB above the average noise level (Fig. 2.4).
- ◇ Open location A.lfg via main menu **Location – Open location**.
- ◇ Overlay a picture from the A.emf file on the window for displaying location areas. To do this, select **Properties** in the context menu of the window, and in the window settings dialog that appears, select graphics import and specify the path to the file (Fig. 2.5).
- ◇ Open the location area settings dialog as described in the User manual, then click the **Load** button and select the A.crg file. In this case, the elements of the list of location areas will be displayed in the list.
- ◇ Perform a test according to the given scheme (Fig. 2.6).
- ◇ Observe location areas in the corresponding window (Fig. 2.7).

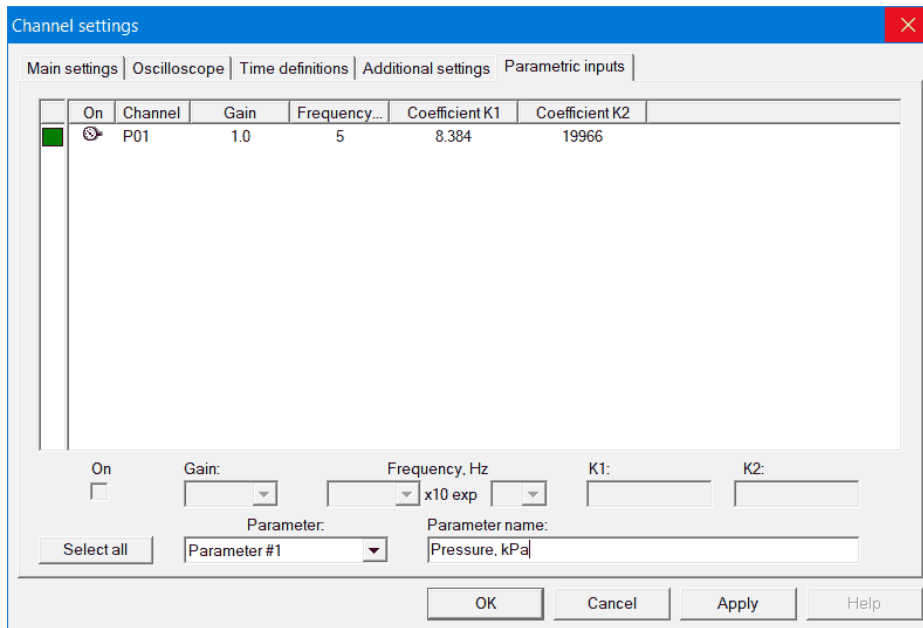


Fig. 2.2. Parameter input settings

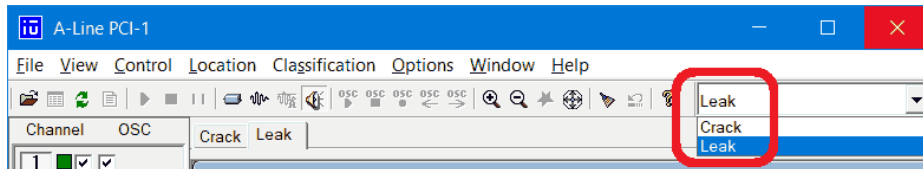


Fig. 2.3. Hardware profiles

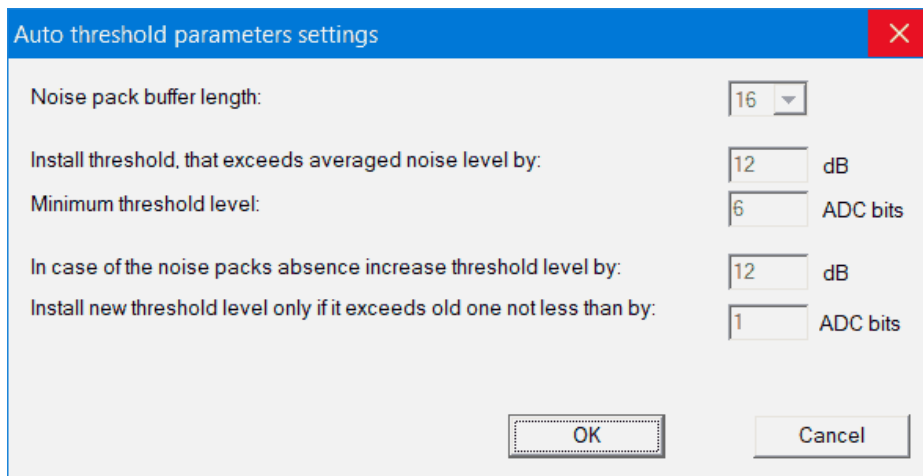


Fig. 2.4. Auto threshold parameters setting

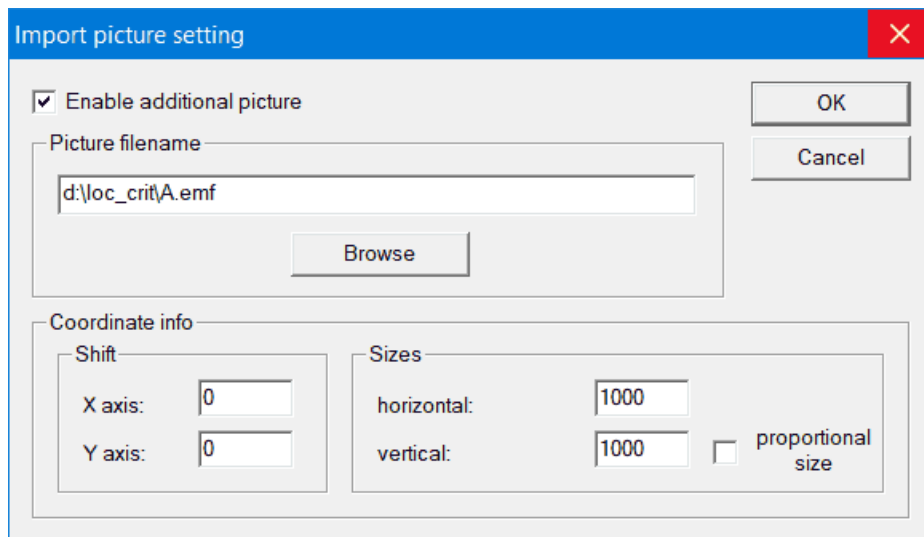


Fig. 2.5. Import picture setting

Pressure graph
($P=12000$ kPa, $V=600$ kPa/s)

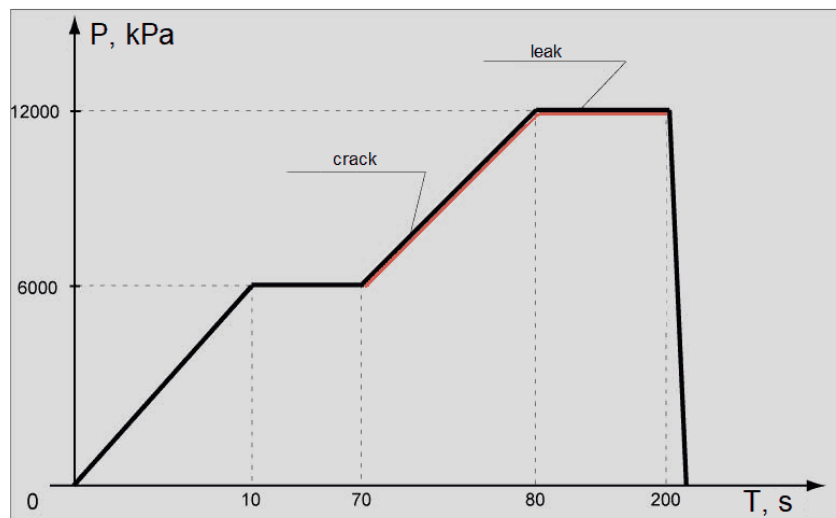


Fig. 2.6. Testing according to a given scheme

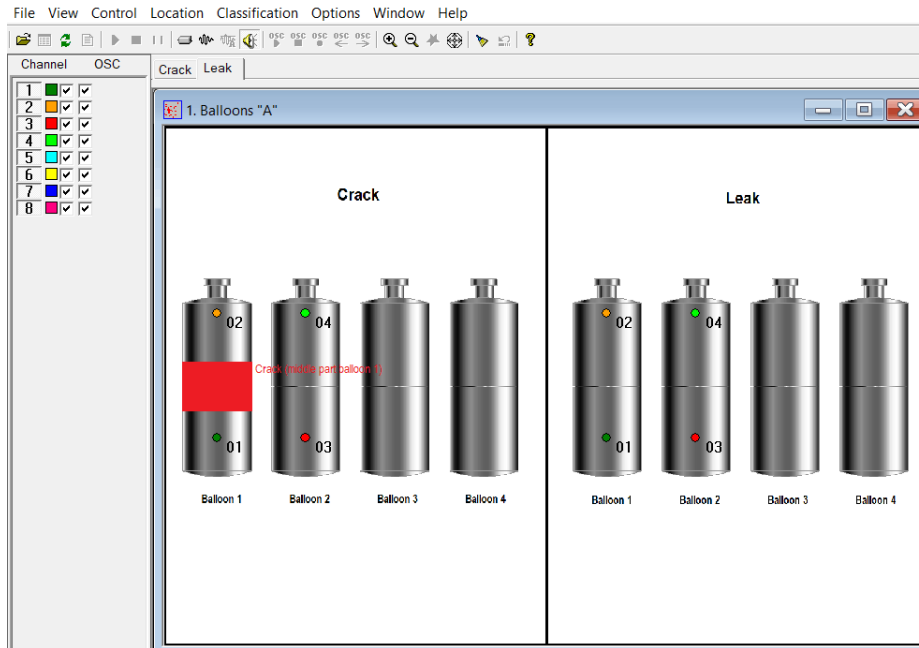


Fig. 2.7. Highlighted location area

The location provided as an example is for testing a cassette of four cylinders. Each cylinder has two sensors. When the load rises from 7.200 to 11 MPa, the “Balloon A (Crack)” location is strobed (Fig. 2.8). In this case, the current profile is "Crack" (Fig. 2.3). When reaching a shelf above 11 MPa, you must manually switch to the "Leak" profile, while strobing the location "Balloon A (Leak)" will be performed (Fig. 2.9). Since the coordinates of the two locations do not intersect, although the same sensor numbers are used, they can be separated in the picture with location areas (Fig. 2.10).

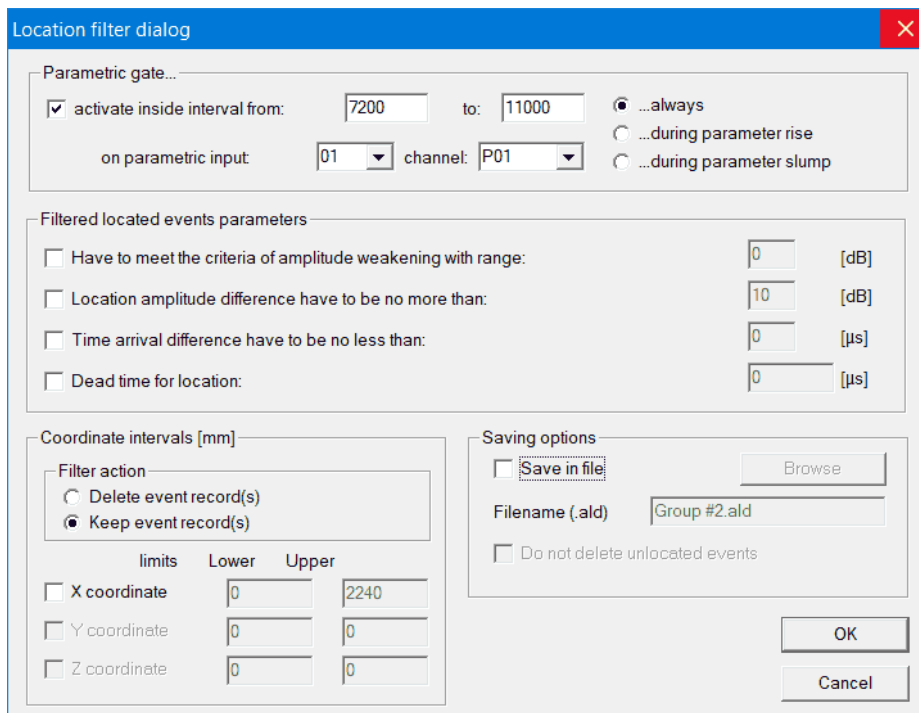


Fig. 2.8. Gating the location. Crack

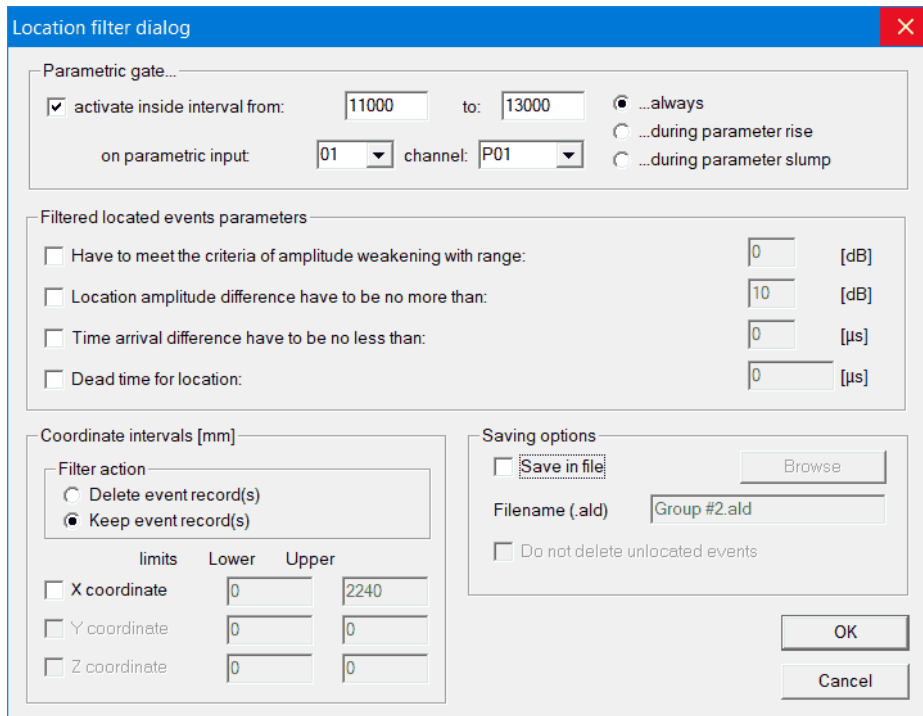


Fig. 2.9. Gating the location. Flow

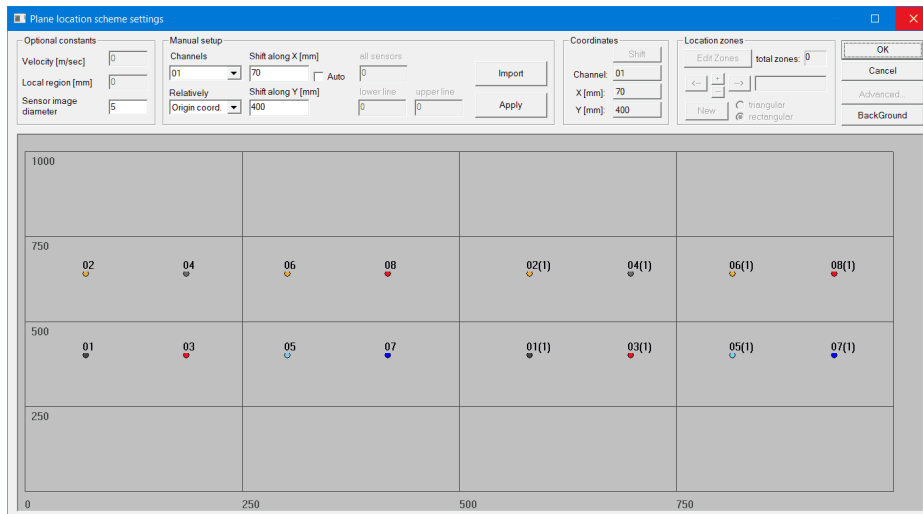


Fig. 2.10. Location scheme settings

The above manipulations for loading the corresponding files can be omitted, but the starting file A.bat can be used. Before start, it needs to be finalized. In the SET PROG_DIR line, specify the folder with the existing version of the A-Line program. In the SET CFG_DIR line, specify the folder where you put the files from the archive. In the SET RUN_DIR line, specify the folder where you want to drop the received data files. In the SET STR2START line, check the name of the program to start (A-Line.exe by default). Then just run this file from explorer.

Each of the elements in the location areas setup dialog has three states, displayed in green, yellow and red colors, depending on the total number of located events. If the specified threshold levels are not reached, then the corresponding quadrangle will not be filled in, and the A.emf background image will be visible.



Chapter 3. Application of the informational statistical AE criterion



Chapter “*Application of the informational statistical AE criterion*” describes and substantiates the application of the informational statistical AE criterion. The corresponding methods are built into the A-Line software by INTERUNIS-IT.

3.1. Description of how it works

At present, when conducting acoustic emission (AE) testing, both in laboratory and in factory conditions, it is possible to obtain enough data to analyze the processes occurring in the material of construction. At the same time, there are a number of problems, the solution of which would make it possible to significantly increase the efficiency of acoustic emission testing and enhance its advantages over other acoustic NDT methods. It is well known that these problems are based on the uncertainty of the source of acoustic emission in time and space, which does not allow one to accurately describe the properties of the acoustic path and, consequently, to reconstruct the form of the wave near this source. The next problem is the irreversibility of most of the processes that generate acoustic emission. Thus, most often, the researcher has only one implementation of the process at his disposal to make a decision.

Nevertheless, the sensitivity of the AE method to the dynamics of processes occurring in the material of a structure when the stress-strain state changes makes it practically indispensable for monitoring the state of an object and predicting its lifetime.

The combination of these problems makes the deterministic approach to their solution untenable. In this regard, the most acceptable are statistical methods for processing AE information, which make it possible to identify the most typical patterns in the development of the process, on the one hand, and to average the effect of statistical outliers, on the other. The efficiency of identifying phenomena occurring in the testing zone, according to acoustic emission testing data, increases significantly if we analyze the behavior over time of not one sign, but two or three in combination.

Based on the threshold principle, the recorded AE data is not a continuous signal, but a sequence of acoustic emission impulse parameters, obtained directly during the experiment or testing, which contains information about the process or set of processes that generate AE. Each impulse is characterized by such parameters as *A* amplitude, *E* energy, *Dur* duration, etc.

These considerations allow us to propose a criterion for detecting the transition from one stage of deformation to another - this is a significant relative change in the statistical characteristics of the distribution of AE impulse parameters. In other words, the moment of transition from one stage of development of damage in the testing zone to another can be determined by the moment of violation of the nature of the AE data flow.

In this case, the most important choice is the identification parameter, which should be both highly sensitive to changes in AE processes, and simple and clear for AE system operators.

Among the traditionally used informative AE parameters, the most physically substantiated is the distribution of amplitudes, which characterizes the degree of randomness of the process. In order to provide access to information about the totality of processes occurring in the testing

object (and for the most correct interpretation of the recorded data), the entire sequence of AE impulses arriving channel by channel is divided into samples. This procedure is done either by a given number of impulses or by a designated time interval. In the first case, each sample contains n AE impulses. In the second case, the sample is formed by those impulses that fell into the corresponding time interval.

The incoming AE data per channel are thus represented by the statistical values of the respective parameters (A , E , Dur , ...). To calculate these values for each channel sample, histograms of these parameters are constructed. Based on these histograms, the main statistics of the resulting distributions are calculated. Among them: average, maximum, distribution mode, and possibly other characteristics.

In the AE-system A-Line by INTERUNIS-IT, time-dependent windows of the real-time type for the main parameters of AE impulses display information in the form of an average value for a given averaging time interval (minimum - one second). A feature of this sampling strategy is the presence of zero statistics at an "empty" second, when no AE impulses were recorded at all. When registering continuous emission, the average values of the parameters will in this case be of a quasi-continuous nature, and this process will be clearly visible on the graphs $A(t)$, $Dur(t)$, etc.

Sampling by the number of impulses also has its own characteristics. The resulting statistics cannot be calculated until the corresponding number of AE impulses has been recorded, which can be whole minutes. On the contrary, with a high activity of AE sources, it is possible to form and calculate a large number of final statistics in one second.

Thus, when calculating, we have either a different temporal sampling density or periodically formed samples with their possible inconsistency due to low AE activity. The study used sampling with a fixed number of impulses n . So far, the question of the sample size remains controversial, since the consistency of statistical estimates depends on it. In this case, it is proposed to solve it as follows:

$$n = \sqrt{N_{\Sigma} / n_{pr}},$$

where N_{Σ} is the total number of impulses in the record, and n_{pr} is the number of expected processes occurring in the testing zone and requiring recognition.

According to the accumulated sample, histograms are constructed for each of the parameters of the AE impulse, incl. amplitude, see fig. 3.1. To create it, the most important parameter is the number of intervals or the number of pockets N_h . This number for the histogram should not be greater than the number of impulses that formed this sample. Then the mentioned statistics are calculated.

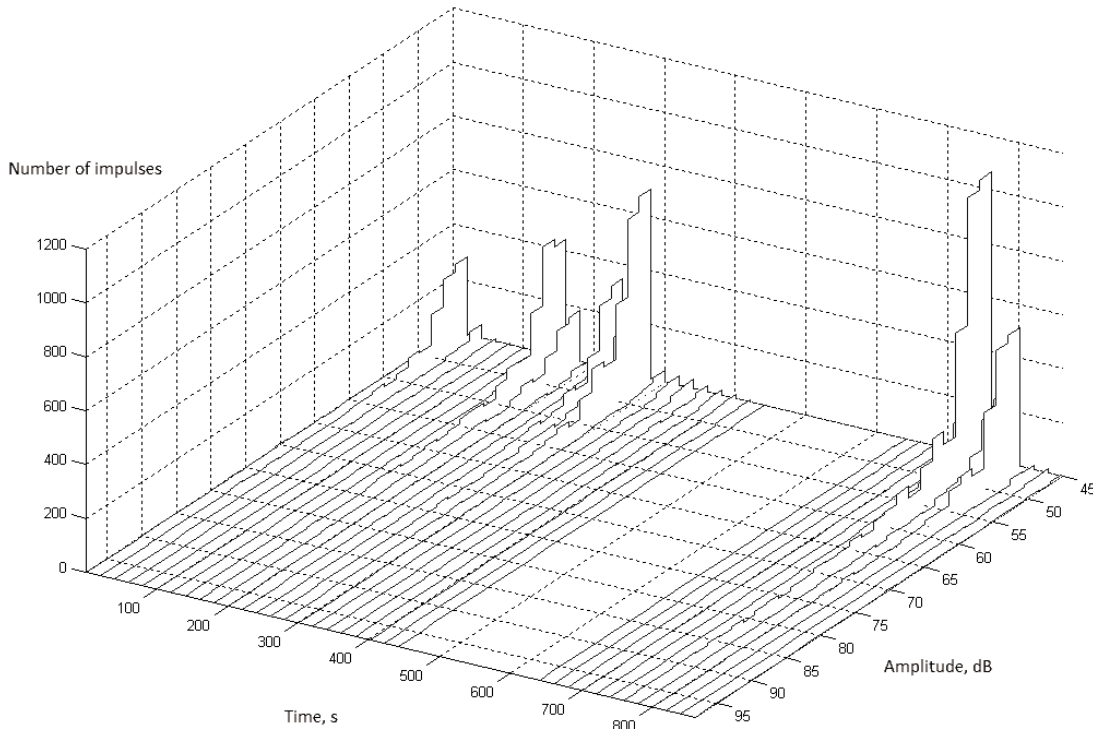


Fig. 3.1. Evolution of the amplitude distribution

The most important characteristic of the resulting histogram is its shape. For distributions close to Gaussian, higher-order moments are usually used. For other distributions, more complex statistics are used. For example, a measure of the similarity of the obtained and exemplary distributions is found. Thus, at the stage of scattered accumulation of microdamages, the AE impulse flow is usually considered to be Poisson. The growth of the main crack is accompanied by a deviation from this distribution. The Builo invariants are constructed on this effect. Therefore, the measure of similarity of the histogram of the time intervals between AE impulses or the amplitude distribution with the exponential one can be considered as an important distribution statistic. Another analysis of the shape of the amplitude distribution was proposed by Japanese experts for the diagnosis of concrete structures, "Ib-value" [1]. The final value is determined by the negative slope of the graph of the cumulative (max-min) amplitude distribution of AE impulses.

Recently, in the works of the "Welding and Testing" and "Interunis" another evaluation characteristic is used - the entropy of the distribution [2], which allows estimating the degree of disorder in the histogram under consideration. Let's consider entropy calculation on the example of amplitude distribution $N(A)$. By normalizing, we obtain the probability density distribution of the amplitudes in the sample, Fig. 3.2:

$$y_i = \frac{N_{Ai}}{\sum_{k=1}^{N_h} N_{Ak}}, \quad i = 1 \dots N_h,$$

from which we obtain an expression for calculating the normalized entropy:

$$S^H = - \frac{\sum_{i=1}^{N_h} (y_i \cdot \ln(y_i))}{\ln(N_h)}$$

Normalization leads to the fact that for an equiprobable process (chaos maximum) with density $y_i = 1/N_h$, $i = 1 \dots N_h$ maximum value will be 1. For a distribution with one realized state (minimum chaos) from N_h , we have zero entropy.

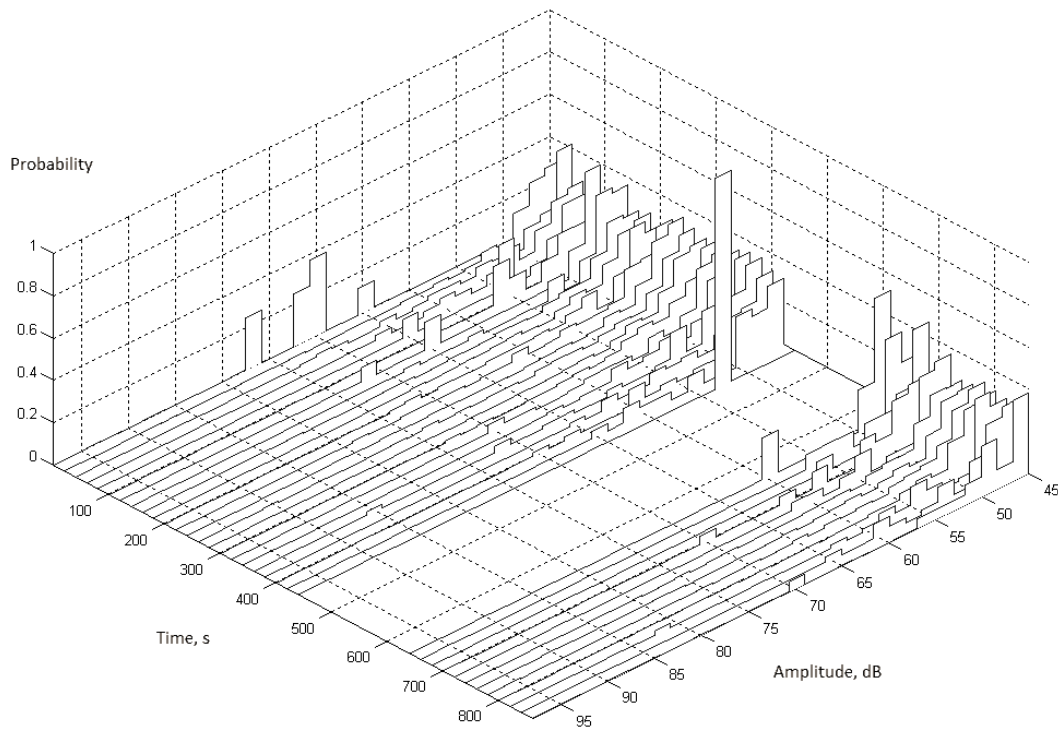


Fig. 3.2. Evolution of the probability density of the amplitude distribution of the process

The disadvantage of entropy is the insensitivity to the sequence of y_i values: at zero entropy, the position of the only realized state is unimportant. However, this is typical when considering one-parameter dependencies, here at least a two-parameter dependence is considered.

Analysis of data obtained both during model experiments and during industrial testing showed that the following dependence can be chosen as an example of an identification parameter:

$$F_{\text{par}} = A_{\text{mod}} (S^H_A)$$

This function F_{par} represents the dependence of the histogram mode of the amplitude distribution A_{mod} on the relative entropy of this distribution S^H_A . The mode is the most frequently occurring amplitude value in the sample. Relative information entropy is a limited function within $[0 \dots 1]$ and characterizes the degree of randomness of a random process.

The entropy of the probability distribution in general, and the amplitude distribution in particular, is an integral parameter and, in accordance with the central limit theorem of probability theory, is asymptotically normally distributed in the flow of AE impulses related to each individual stage of deformation and destruction. This is confirmed by the results of the analysis of time series of AE data.

The results of calculations by channels are highlighted in the appropriate color and plotted on the graph in the specified coordinates, resulting in a diagnostic diagram. Source identification can be carried out by the position of groups of points on the diagram field.

The module for calculating the statistical diagnostic graph is built into the standard program of the A-Line system and is available for download from the site. The settings dialog provides the ability to select the type of sampling (by number and time), the parameter of AE impulses for analysis, and the ability to save calculation results to a file.

3.2. Application examples

Trace the possible position of a point on the plane in the coordinates " $S_A^H - A_{mod}$ " for possible processes in fig. 3.3...3.7.

Fig. 3.3 shows a diagnostic diagram of nitrogen loading of a ball tank 1-10 for storing butadiene. This object did not contain active sources. The registered AE impulses in the diagram are localized in zone I. This zone is characterized by the spread of entropy S_A^H in the range (0.3 ... 0.7), and the modal (predominant) value of the amplitude lies above the threshold value by 0-5 dB. In fact, the AE impulses that formed these statistical points are the noise of the object during pressing (practically the Poisson process), subject to an exponential distribution. The location of such impulses usually represents location points randomly scattered over the surface of the object.

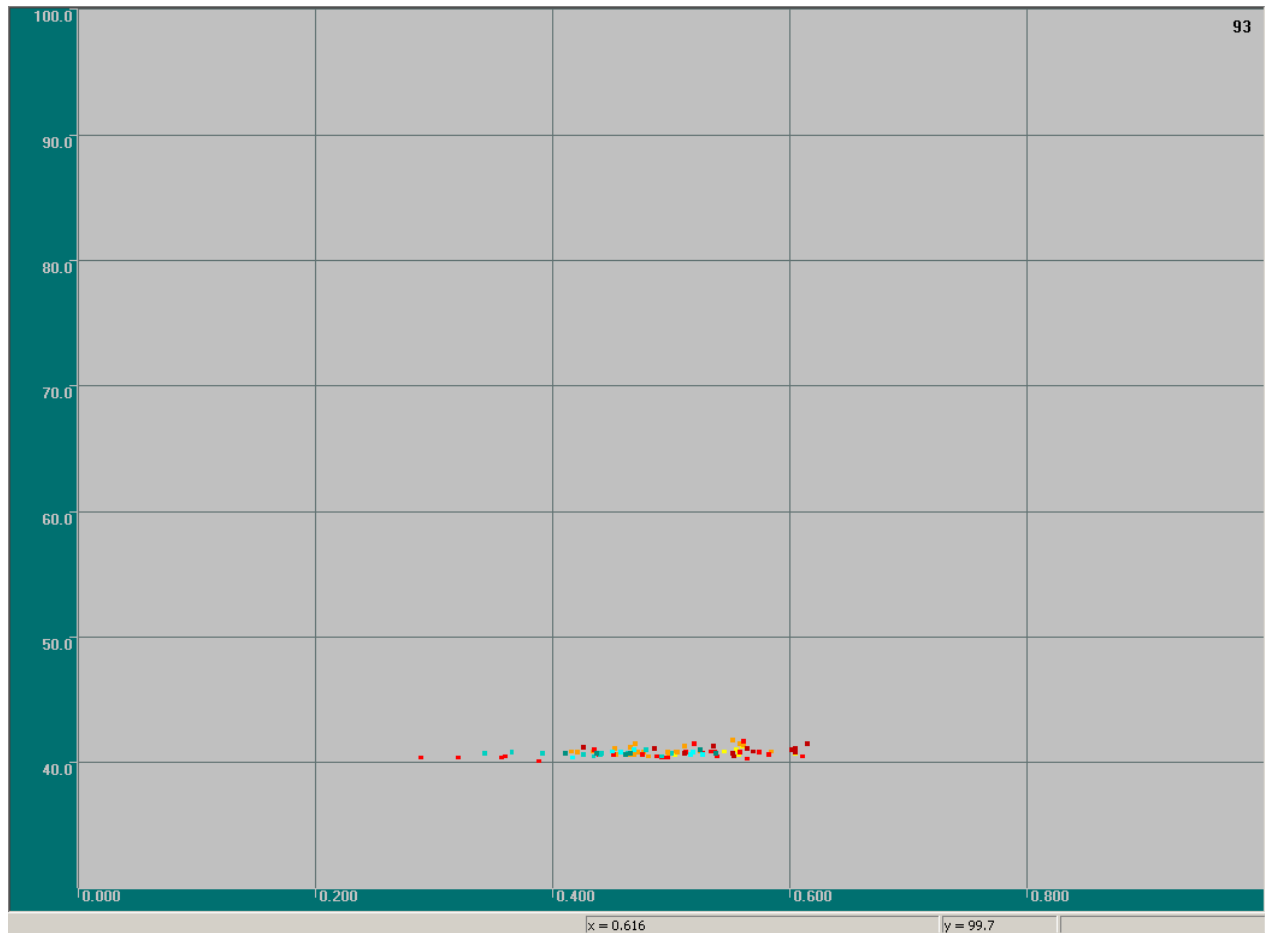


Fig. 3.3. Diagnostic load diagram of a defect-free object

Fig. 3.4 shows a diagnostic diagram of nitrogen loading of a ball tank 33-1 for storing butadiene. A class II (active) source was found at this object. The recorded AE impulses during loading of the object are localized in the diagram in zones I, II, and III. Noise zone I is a kind of benchmark against which other zones stand out.

Zone II stands out against the background of zone I both by the modal value of the amplitude and by the entropy, occupying an interval of 0.4 (see also fig. 3.5) to 0.8. These statistical points are obtained due to the fact that those impulses whose amplitude is above the threshold begin to dominate in the noise stream. It is due to this that the modal value of the amplitude increases. Thus, the mode position of the points corresponds to the degree of source activity, and at low activity, the mode will again fall to the threshold noise value. In addition, a significant increase in the prevailing recorded amplitudes leads to the fact that the mode value can rise to values in excess of 90 dB (see Fig. 3.6 and Fig. 3.7). Entropy, on the other hand, increases due to the fact that the spread of amplitude values becomes wider, and accordingly, the degree of chaos also increases.

Zone III corresponds to AE impulses typical of leaks. This zone is characterized by the entropy spread S_A^n in the range (0.0...0.3), the modal value of the amplitude is equal to or higher than threshold value. So, with an increase in pressure in an object containing discontinuities, the leaky signal in its amplitude also increases almost synchronously. And when the leak signal reaches the amplitude of the threshold value on the diagnostic diagram, statistical points fall out in zone III with a modal amplitude equal to the threshold. A further increase in the amplitude of the leak signal leads to the rise of the precipitation points along the diagram up to the corresponding modal value.

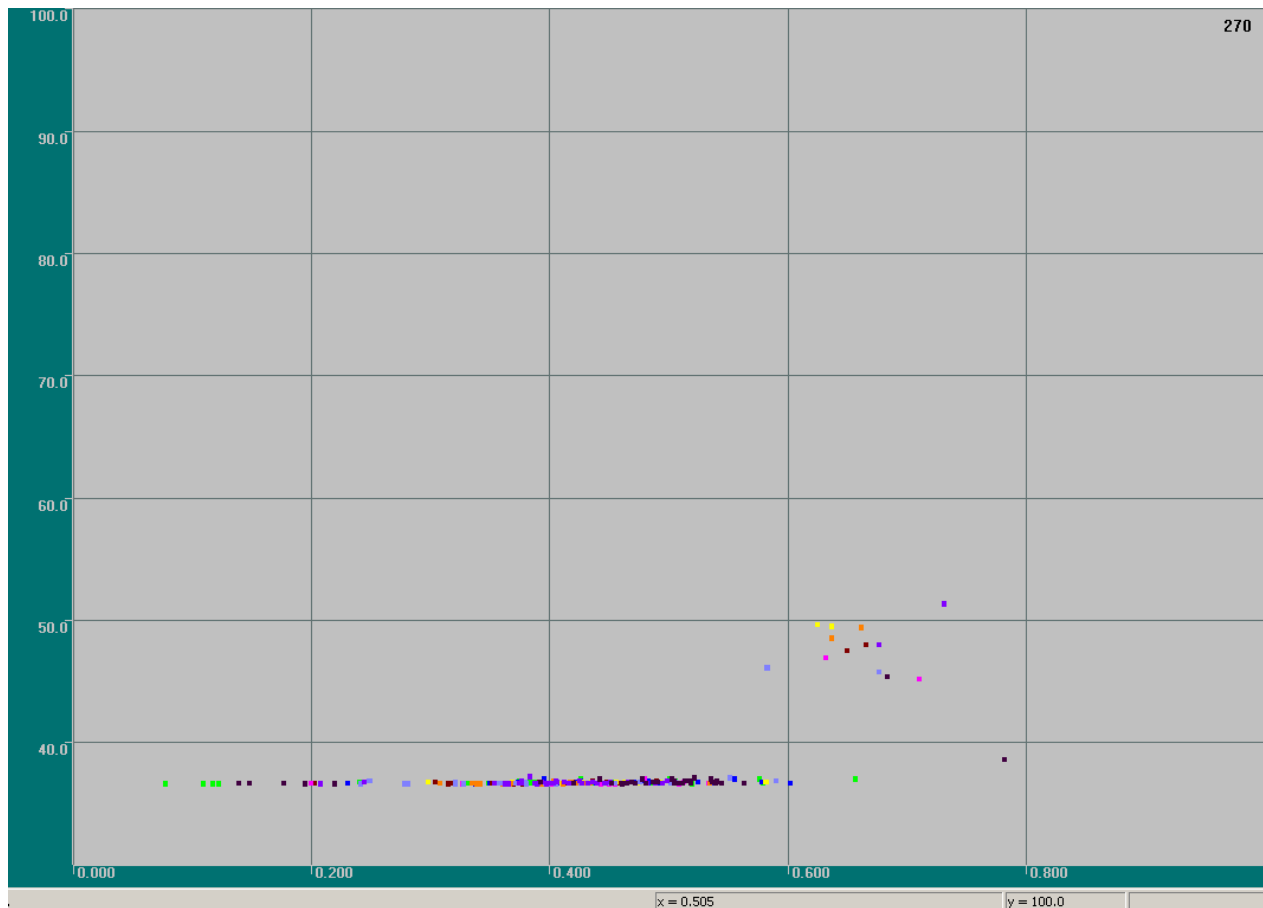


Fig. 3.4. Diagnostic loading diagram of an object with class II source (active)

Figure 3.5 shows a diagnostic diagram for loading a railway tank with air. The threshold is floating. A hole of the order of 1 mm was found. Since the threshold level for each channel was set depending on the average noise level, the localization on the diagram also has a stepped character. However, the entropy value lies within (0.0...0.3), as in the diagram in Fig. 3.4. The different average signal level for the channels is apparently associated with attenuation: the farther from the hole, the lower this value.

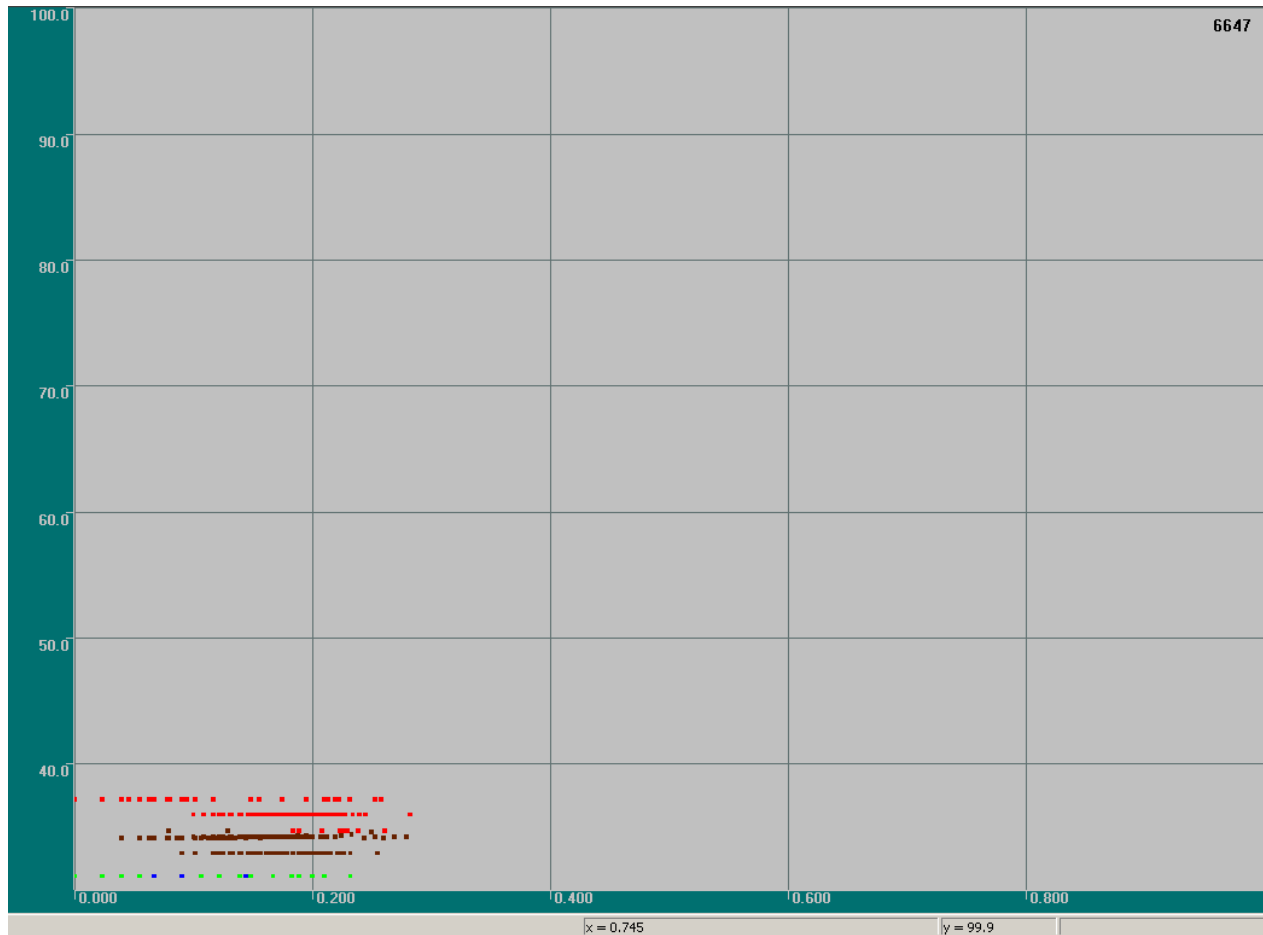


Fig. 3.5. Diagnostic flow chart

Fig. 3.6 shows a diagnostic diagram of cyclic loading of a reference sample and bringing it to failure. The appearance of zone III on this diagram could be explained by the flow process, however, by definition, there was no penetration of the working medium through the discontinuity. A possible explanation for this phenomenon may be the phenomenon of plastic deformation, accompanied by AE impulses with a small (near-threshold) amplitude. As a result, the background noise process with an exponential distribution literally dissolves into a distribution with the only possible near-threshold state from plastic deformation.

Zone II begins to be identified in the experiment with the growth of "whiskers", V-shaped cracks in the narrow section of the sample. Zone IV is the last zone that appears on the diagnostic diagram, corresponds to the critical growth of a crack (main crack) just before the destruction of the sample.

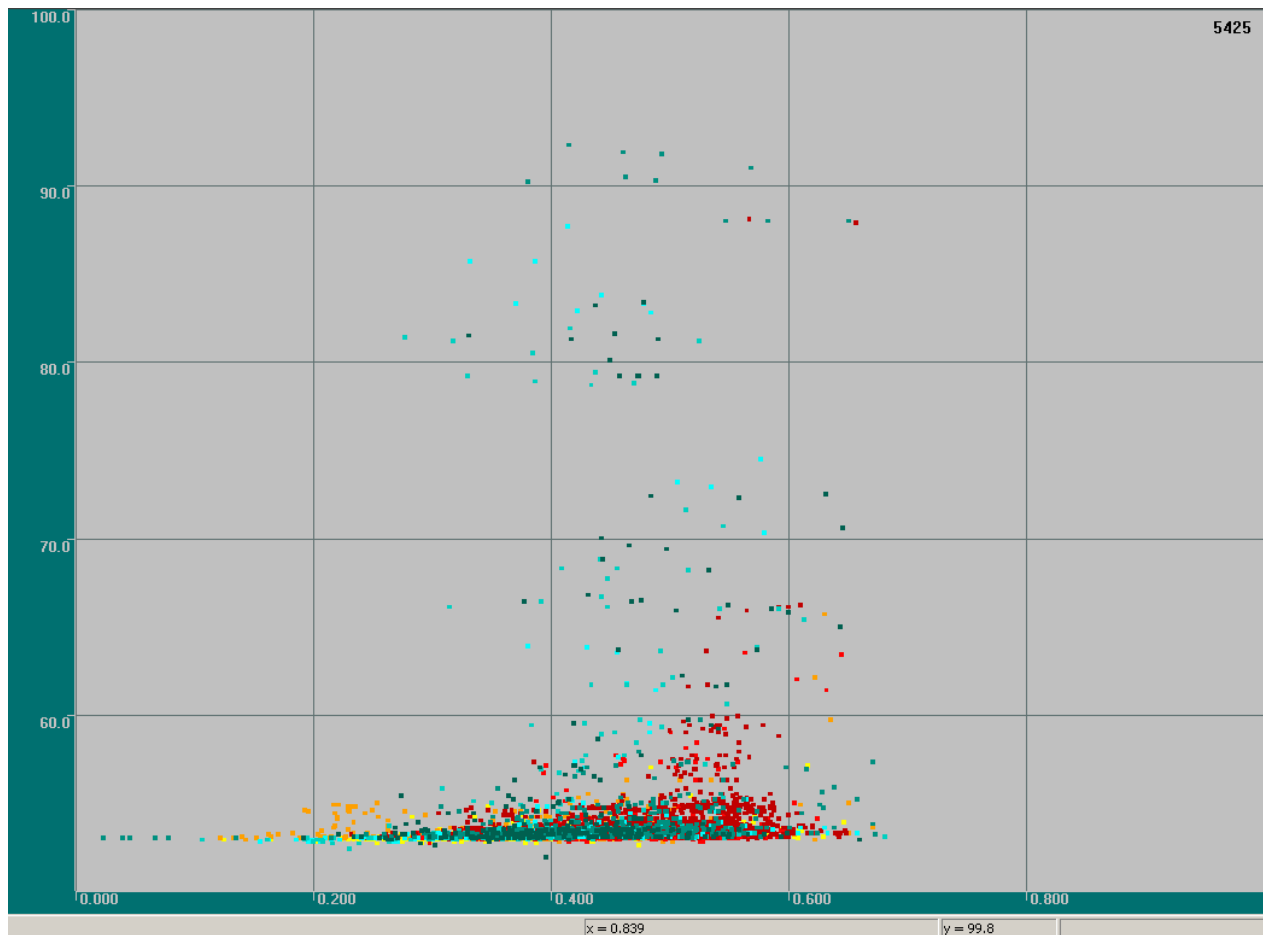


Fig. 3.6. Diagnostic diagram of cyclic loading of a standard sample and bringing it to failure

Fig. 3.7 shows a diagnostic diagram for bringing a concrete slab to failure with a size of 4200 X 1700 X 160 mm. The loading was carried out by lowering special reinforced concrete blocks onto the slab.

When testing, the points fell into two zones, I and II, and at the final stage, preceding the destruction of the plate, zone IV was designated. When comparing Fig. 3.6 and Fig. 3.7 there is direct analogy, except for zone III.

As a result, it can be stated that during the destruction of the testing objects (reinforced concrete slabs under repeated statics and a metal sample under cyclic loading), the statistical diagram has a similar form, and the resulting points on this diagram alternately fill zones I, II and IV, and before the destruction of the object, zone IV appears - a zone from the formation of main cracks.

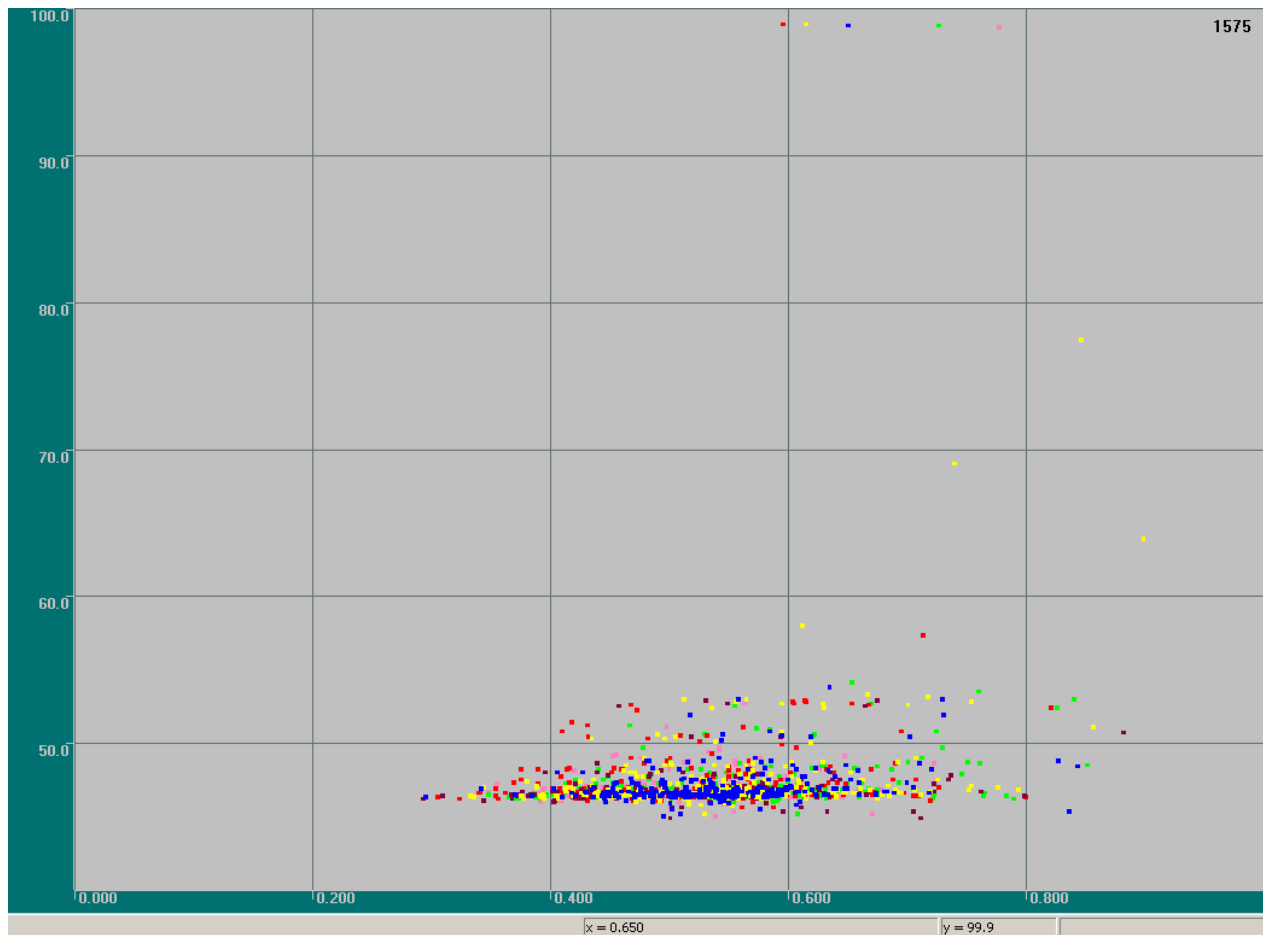


Fig. 3.7. Diagnostic diagram for bringing a concrete slab to failure

3.3. Conclusions

1. The possibility of identifying types of defects (accumulation of scattered microdamages, growth of main cracks, leaks) by a combination of features (AE impulse amplitude mode; amplitude probability distribution entropy) has been experimentally confirmed.
2. It has been established that the beginning of the destruction process can be judged by the dynamics of the movement of statistical points on the diagnostic diagram $A_{\text{mod}}(S_A^n)$ from zone III to zone IV at the non-stationary phase of defect development.

3.4. References

1. Shiotani, Nakanishi, Luo, Haya, Noda. Damage assessment in railway sub-structures deteriorated using AE technique. Research Institute of Technology, Railway Technical Research Institute (Japan).
2. Ship V.V., Muravin G.B., Samoiloa I.S., Dorokhova E.G. The application of complex information parameter to acoustic emission for diagnostic during the stage of fracture.- Nondestr. Test. Eval., 1997, V.13, pp. 57-71.



Chapter 4. Arbitrary antenna fuzzy locating (AAFL)



Chapter “*Arbitrary antenna fuzzy locating (AAFL)*” is entirely devoted to fuzzy location.

4.1. Differences between the AAFL method and location with triangular and quadrangular antennas (LA3 and LA4)

Table 4.1.

LA3 and LA4	AAFL
There are restrictions on the installation of sensors on the object, due to the location algorithm.	Restrictions on the installation of sensors at the facility are less stringent, and will be lifted in the future.
It is necessary to set location triangles (LA3) and location quadrilaterals (LA4); location is made only by them.	There is no need to do any artificial division of the object into sections for location. It is enough to place sensors on the object.
The only velocity of elastic waves propagation over the surface of the testing object is set.	The range of elastic wave propagation velocities over the surface of the testing object is set, which is more realistic.
Location is performed only using sensors at the tops of the location sections, i.e. e. only for three (LA3) or only four (LA4) impulses from each pack, and only for such triplets (quadruples) of impulses that came to the sensors at the vertices of any location area.	Location is performed by an arbitrary number of any impulses in a pack (from two or more); only the maximum number of impulses in a pack used for location is set.

LA3 and LA4	AAFL
Location is performed by approximation triangles (LA3) or by approximation flat quadrangles (LA4), which leads to significant distortions and related errors on the curved sections of the object.	Location is performed taking into account the real geometric shape of the object, which reduces distortion and related errors to a minimum; which requires, however, a more accurate description of the geometric shape of the object and the setting of all relevant parameters.
The result of location by one pack of impulses is one point on the object, which almost always differs from the location of the source due to various errors, while the location error is not evaluated.	The result of location by one pack of impulses is the area on the object in which the source is located with a high probability.
The result of location by multiple packs is a set of points on an object, among which there are many random ones and it is not always easy to select those points that represent useful information.	The result of location by multiple packs of impulses is a set of areas on the object, the intersection of which with each other makes it easy to detect relatively small areas in which the source is located with a very high probability.

4.2. Short explanation of the AAFL method

The Arbitrary antenna fuzzy locating (AAFL) method consists in calculating for each pack of impulses on the object an area consisting of all possible points where such an event could occur that could create a given pack of impulses with a given arrangement of sensors and a given the range of elastic wave propagation velocities over the surface of the object. To do this, the surface of the object is modeled by a discrete network of a finite number of points, and for each pack of impulses, all nodes of this network are calculated, in the vicinity of which an event could theoretically occur that creates this pack. The list of all such nodes is the description of the location area for this pack.

The location is fuzzy, because for each pack, not one point on the object is indicated, but an area. However, a single location point cannot be calculated without error, so this fuzzy method is more accurate than a point location, since the desired event source is located in the output area with a high probability. The intersection of the location areas obtained for different packs makes it possible to more accurately determine the location of the source, provided that several packs of impulses were received from one source. When depicting areas on an object in the **A-Line** program, the overlapping areas of the location areas are painted in different colors, depending on how many areas overlap in this area, and the user can set the color dependence on the number of overlapping areas.

To complete the picture, it should also be clarified that for the location in each pack of impulses, not all impulses of this pack are usually used, but only the first few, since later impulses are usually weaker and can be distorted, and therefore can worsen the location. In addition, in order for these first few impulses to be more likely to be of high quality, packs containing a sufficiently large number of impulses are usually selected, and location is already made from these packs (according to the first few impulses from each). Both parameters (the minimum number of impulses in a pack used for locating and the maximum number of impulses used for locating from each pack) can be set by the user.

And the last. There are “bad” packs in terms of location, which are located, but very inaccurately, that is, a very large area. The maximum area size can be limited by the user, and it is recommended to do this in order to avoid large uninformative areas that worsen the overall location picture, as well as to avoid too long (but uninformative) calculations of these large areas. In addition, the user can set the size of the elementary cell of the lattice that models the surface of the object, that is, the characteristic distance between neighboring nodes of this lattice. The smaller this size, the more detailed the drawing of each area will be, but the longer the calculation will be.

Specific recommendations for setting all the described parameters are contained in the following brief guide to using the AAFL method.

4.3. A quick guide to using the AAFL method

In order to locate using the AAFL method, you must set the following parameters:

- ✧ precise description of the geometric shape of the object;
- ✧ list of channels (sensors) used for location and location of sensors on the object (including error!);
- ✧ range of elastic wave propagation velocities on the object;
- ✧ the size of the elementary cell of the lattice and the maximum allowable size of the area obtained during location;
- ✧ the minimum number of impulses in a pack used for location and the maximum number of these impulses used for location.

In addition, it is desirable to select clustering parameters in a certain way. Below is a brief explanation and initial recommendations for each of these points. Currently, this type of location is implemented for the sphere, so everything is explained using the example of the location of the sphere.

An accurate description of the object's geometric shape

For a sphere, it is enough to set the radius (diameter) in the **Location scheme settings** dialog box (menu **Location – New location** or **Location – Edit current location**).

Channel settings

For this type of location, it is enough to indicate the channels participating in the location and their location, no location triangles or quadrangles need to be specified. The coordinates of sensors for a given type of location in the case of a sphere is specified in the following format. The equator and the zero meridian are determined on the sphere, and then for each sensor are indicated:

- ✧ **longitude** is distance (in millimeters!) along the equator from the zero meridian to the meridian, on which the sensor is located (it is possible with the sign **+** in one direction, **-** in the other);
- ✧ **latitude** is distance (in millimeters) from the sensor to the equator, with **+** sign if the sensor is above the equator, and sign **-** if below;
- ✧ **error** is error in determining the coordinates of the sensor (in millimeters).

The sensor installation error must be specified to enhance the location accuracy: the more accurately the location of the sensors is known (the smaller the error), the more accurate the location of each pack of impulses will be (that is, the smaller the size of the located regions

and the resulting location areas), but with an incorrect indication coordinates of the sensors (for example, if the actual error of their installation is greater than the specified one), the location may be performed incorrectly or not work at all.

You can specify the channels participating in the location in the usual way in the **Select channels for sphere location scheme** dialog (using the **Select** button in the **Location scheme settings** dialog). In the same place, select **optional** from the list **Involute method** to select this type of location. After that, in the dialog for setting the location parameters (using the button **Details** in the dialog **Location scheme settings**), you need to set the longitude, latitude and error of each sensor in the format described above.

Selection of velocity range

Until now, for the location, a single velocity of propagation of elastic waves over the surface of an object was set. This is not realistic for several reasons, the main ones being:

- ◇ 1) An elastic wave consists of different modes (that is, elastic waves of different types), each of which has its own velocity under given specific conditions. Thus, there is physically no single velocity of propagation of elastic waves over the surface of an object, there is only a set of different velocities for elastic waves of different types. Different channels (and even the same channel for different impulses) can register the arrival of different modes, depending on which of them is less attenuated or distorted on the way from a given source to a given sensor.
- ◇ 2) The main method of recording impulses now is to register by the channel the moment when the amplitude of the transmitted wave exceeds a certain specified threshold, which is set for each channel depending on the overall noise level in a given section of the object. Therefore, channels can register not only the arrival of different elastic wave modes, but also different components of these modes (depending on the threshold), which also changes the actual velocity of elastic wave propagation from the event source to a particular sensor.
- ◇ 3) The object usually has many small unaccounted structural features, such as seams, hatches, nozzles and other geometry distortions, which make the propagation paths of elastic waves rather complicated, thereby changing the actual wave propagation velocity compared to the calculated model object.
- ◇ 4) Anisotropy of the material is possible on the object, and therefore elastic waves can propagate at different velocities in different parts of the object and in different directions.

All of the above gives reason to believe that it is more realistic to set not one velocity, but a whole range of elastic wave propagation velocities on the object, and to carry out location, taking into account that the exact propagation velocity of each wave is unknown, but must be in the specified range. For example, usually the velocity of elastic waves in a metal was set approximately equal to 3000 m/s. Instead, with this type of location, you can specify a range from 2700 m/s to 3300 m/s, since it is in this range that the velocities of different modes usually lie when they are measured more carefully.

It should be noted that specifying a wider range (“with a margin”) makes the location more likely, but the size of the located areas will increase, that is, the location becomes more fuzzy. Reducing the range makes the location more accurate, but the possibility of error increases when the found areas do not contain the source due to the fact that the real wave velocities do not lie in the specified range. It is recommended to choose a range based primarily on the knowledge of wave propagation velocities in a given material, not trying to “improve” the location by unreasonably narrowing the range, as this leads to location errors.

You can set the range of velocities, that is, the minimum and maximum velocities, in the same dialog for setting the location parameters, where the coordinates of the sensors are set (by the button **Details** in the dialog box **Location scheme settings**).

Setting the lattice parameters

The size of an elementary cell of a lattice is the approximate distance between adjacent nodes of the lattice, which is used to model the surface of an object. The smaller this size, the more accurate the rendering of the location areas, but the calculation time increases approximately inversely with the square of the given size, that is, for example, by making this size half as large, you can slow down the algorithm by about four times. It is recommended to start by setting the cell size to tens of millimeters, and then it can be increased if the calculation is too slow, or reduced, for example, for small objects. If this size is made too large, then the location areas will look too schematic, but the greater accuracy of drawing these areas is also usually useless, since they still only approximately describe the location of the source. A cell size of 10 mm is almost always sufficient, but to velocity up calculations for large objects, it is better to start with 30 mm.

Another parameter associated with this size is the maximum allowable area size. Areas larger than this size are culled when locating. The maximum area size is now set by the number of elementary cells of the lattice. For example, if the unit cell size is 10 mm, then setting the maximum allowable size to 100000 will reject areas larger than approximately 10 m^2 (because each cell will have match approximately 1 cm^2). If the unit cell size is 30 mm, then there will be approximately 1000 cells in an area of 1 m^2 and to reject areas larger than approximately 10 m^2 , you need to set the maximum area size to 1000. In the future, it is planned to be able to set the maximum allowable area size immediately in units of area.

Which areas should be culled? The approximate diameter of the maximum area with a good location on 3-4 sensors is equal to the distance between adjacent (nearby) sensors on the object, multiplied by the percentage range of velocities (that is, the ratio of the difference between the minimum and maximum velocities, divided by the average between them). This is the maximum theoretically possible area, in practice they are smaller, and when locating with a large number of sensors, even less, but to set the maximum allowable area size, you should focus on the maximum theoretical size. For example, if the distance between nearby sensors on an object is 6-8 m, the minimum velocity is 2700 m/s, and the maximum velocity is 3300 m/s, then the percentage spread of velocities is 20%, and the approximate diameter of the maximum location area for one packs will be equal to $8\text{m} * 20\% = 1.6 \text{ m}$, that is, the area of the maximum area is about $2\text{-}3 \text{ m}^2$. This is the maximum theoretical size of the location area, but the size of the maximum allowable area should be set several times larger, for example, in this case 10 m^2 (in terms of the number of elementary cells, depending on the size of one cell).

In principle, an unjustified increase in the size of the maximum allowable area does not have negative consequences for the location, it only increases the calculation time if a very “bad” packet is found, which is located by a very large area, such cases are rare, and only to cut them off, we introduced this setting. If, on the contrary, this parameter is made too small, many useful and informative areas can be rejected. Therefore, the maximum allowable area size should be set with a several-fold margin, cutting off only areas that are clearly too large in size, many times greater than the expected size of the location areas. You can set the unit cell size and the maximum allowable area size in the **Advanced location options** dialog box in the **Optional location parameters** group, called by the **Advanced** in the location settings dialog.

Setting pack options

Fuzzy location is based on impulse packs, that is, groups of impulses whose proximity in time suggests that they could come from a single source. Packets of impulses are found automatically, you only need to set **Distinctive object size**, that is the maximum possible distance between two points on the surface of the object. This can be done in the **Parameters of AE-pulses pack** dialog, called by the **Parameters** button in the **Advanced location options** dialog box.

Fuzzy location can be performed not only by three or four impulses from each pack, but by a larger number, this number can be set by the user. This number is the maximum number of packs used for location. The fact is that for a larger number of impulses, location is performed more accurately and more reliably, but only on condition that all these impulses are of sufficient quality, they are not too noisy and not too damp. To increase the likelihood that all impulses used for locating will be of good quality, only those packs in which the total number of impulses is greater than what is used for locating can be used. For example, you can use only packs containing 10 or more impulses, but locate only the first five impulses from each such pack. The minimum number of impulses in a pack used for location is also set by the user.

Which packs to choose and how many impulses to locate depends on the quality of the data. If the impulses are powerful, and the impulses come to many sensors at once, then you can choose packs of 10-12 impulses, and locate 6-8 impulses, while most likely there will be no false locations. If the impulses are weak, and there are few impulses in the packs, it is necessary to locate by 3-4 impulses, while fuzzy location is still much more reliable and clearer than point, but experience shows that even when locating by 4 impulses, there are cases false location. The point is that the regions corresponding to a small number of impulses are not simply connected, that is, they consist of more than one connected component. Currently, the fuzzy location algorithm in such cases finds only one connected component for each pack, so there are cases when a false area is found. This can happen, for example, when the sensors, according to which the location of a given pack is made, line up approximately on the same straight line (or, in the case of a sphere, on the same arc of large radius), then two possible areas of location are located on opposite sides of this line, and without additional data (for example, an impulse from some sensor that does not lie on this line), it is impossible to determine which of the two areas is correct.

A general recommendation is to first use packs containing at least 8 impulses and locate by 4. Then, if the data is good and there are a lot of such packs, increase both parameters, that is, locate by 5-6, for very good data by 7-8 impulses, and at the same time take packs that contain 10-12 impulses or more (if there were more sensors at the facility). In any case, if a probable source is found, then its location should be carried out using at least 5-6 sensors to exclude false location. If the data is bad, and there are few packs, then you need to take packs of 5-6 impulses, locate by 3, but if a possible source is found, try to locate the packs corresponding to it by a larger number of impulses, for this you can first view the corresponding packs in the data view window and determine, by the parameters of the impulses, how many of them are of high quality, suitable for location. Both of these parameters can be set in the **Advanced location options** dialog box in the **Optional location parameters** group, called by the **Advanced...** button in location settings dialog.

Configuring clustering options

To configure the visual displaying of the results in the **Location scheme settings** dialog box, in the **Clustering legend** group, by pressing the **Change settings** button, you can open the dialog **Clusterization settings**. There, in the section **Carry out clusterization**, it is recommended to select the item **through % of events in the cluster relatively accumulated maximum events number**, and then make the custom five intervals as follows:

- ✧ first interval: from 1 to 20;
- ✧ second interval: from 21 to 40;
- ✧ third interval: from 41 to 60;
- ✧ fourth interval: from 61 to 80;
- ✧ fifth interval: over 80.

In this case, the intersection areas of the location areas will be automatically highlighted in color on the image of the 3D model of the location.

4.4. AAFL example

For clarity of the above, we will consider here just one example of comparing locations by different methods. As a data file, data from the calibrator was used, which was used as the third of 14 sensors located on the sphere.

- ◇ Normal location with a triangular antenna without pack filtering.

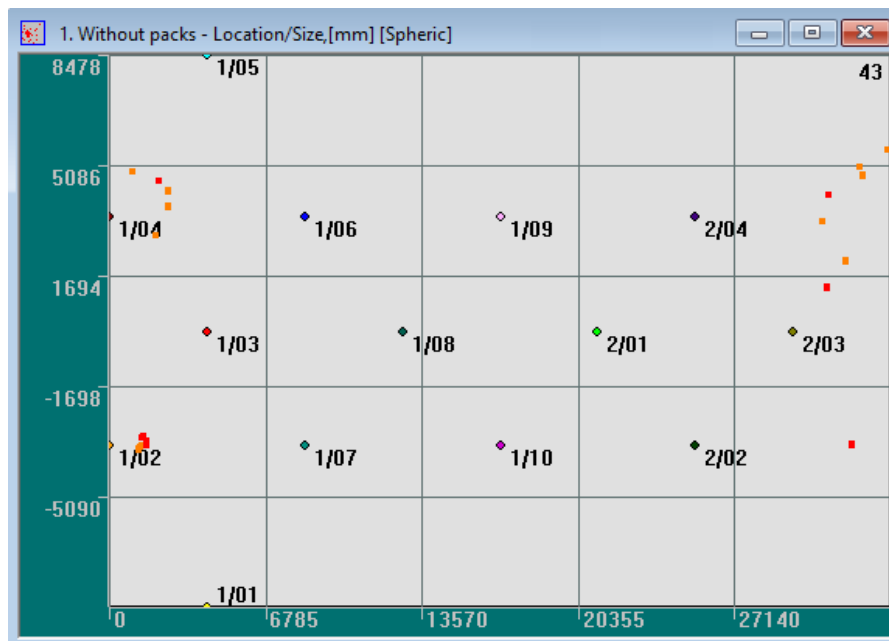


Fig. 4.1. Locating with triangular antenna without pack filtering

- ◇ Location with pack filtering.

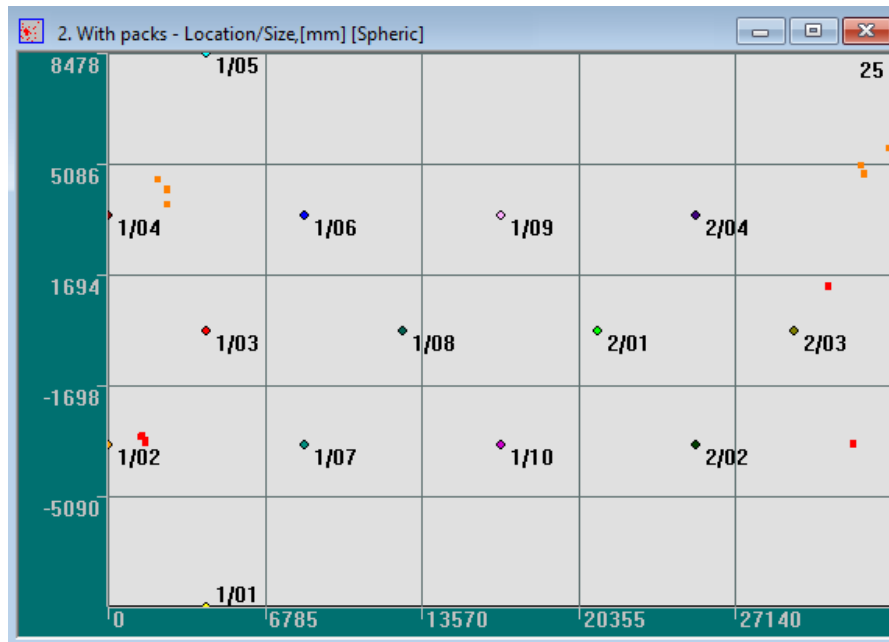


Fig. 4.2. Location with pack filtering

◇ Fuzzy location in packs.

Let's consider an example of fuzzy location by packs with at least 8 impulses, of which the location was carried out by 4 impulses (let's denote it imp8/4, these are the recommended parameters for the very first, one might say, approximate, location). Only 12 out of 14 sensors were used in this location: sensors located near the poles were not used in this location, because their location was not known accurately, and their use would only worsen the location accuracy due to a large error.

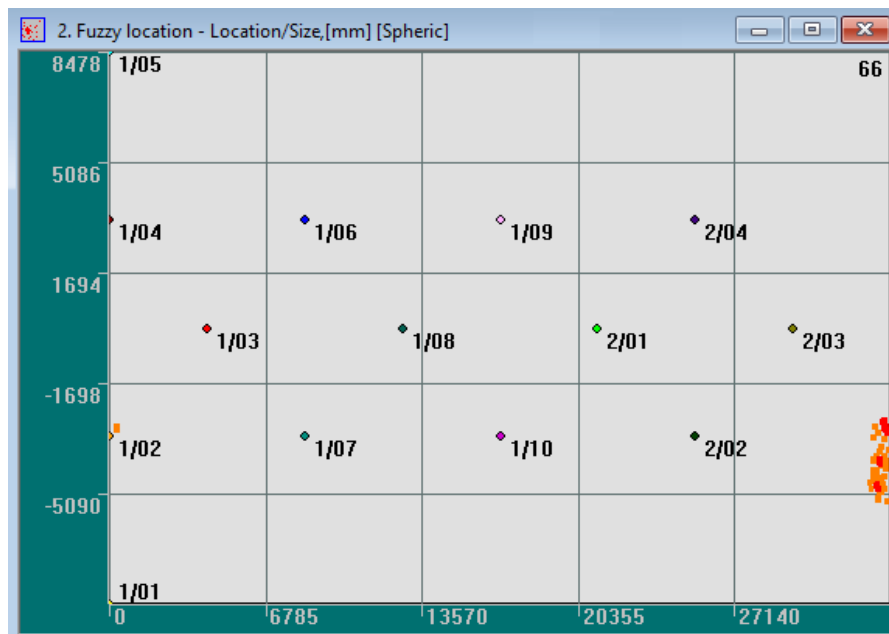


Fig. 4.3. Fuzzy location by packs (AAFL)

As you can see, in the third case, the location is the most accurate and contains significantly fewer false points. But on a flat net of the object, only the centers of the regions are shown. The difference is even clearer in the image of the volumetric model, it is in it that the location areas are depicted. Here is the location with pack filtering:

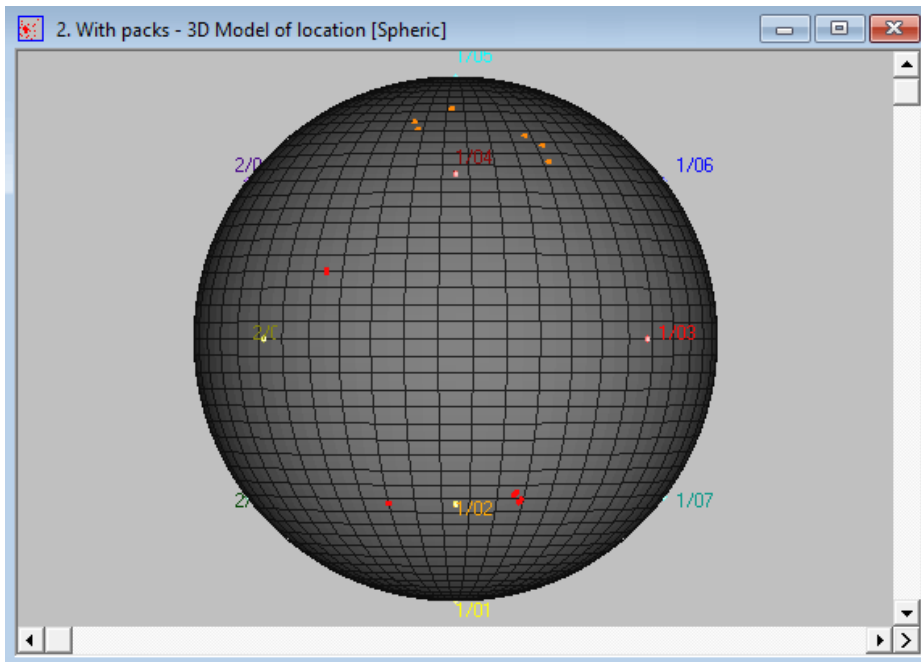


Fig. 4.4. Location with pack filtering (imp8/4), front view (3D model)

The same, rear view:

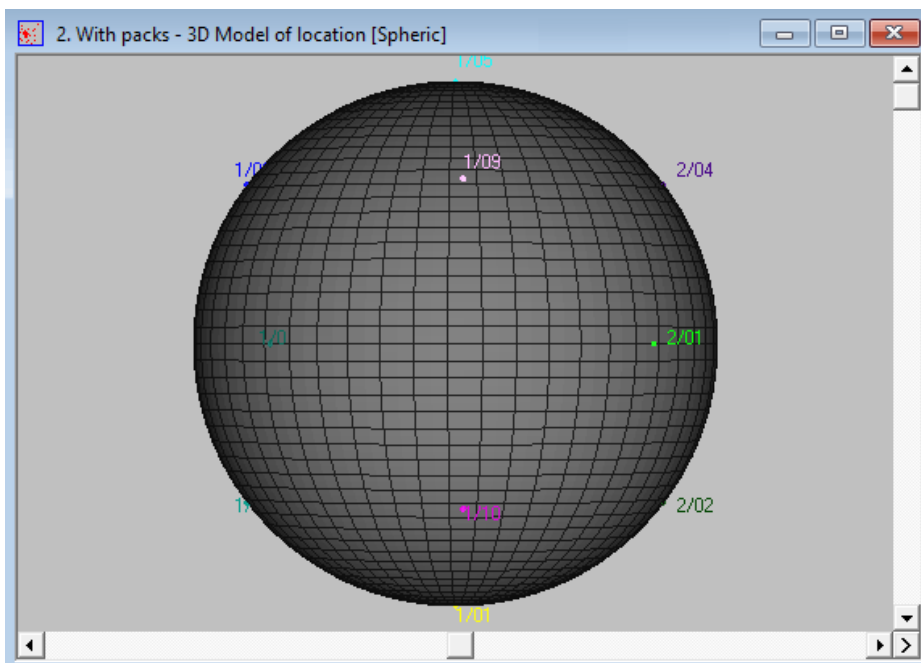


Fig. 4.5. Location with pack filtering (imp8/4), rear view (3D model)

And here is the location using the AAFL method, with the same initial parameters (imp8/4):

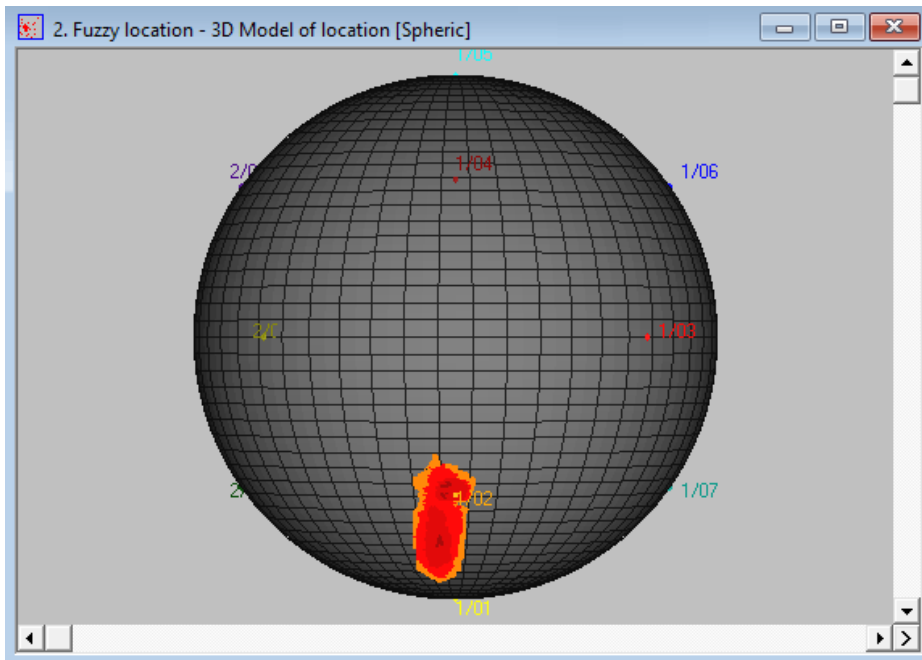


Fig. 4.6. Fuzzy location by packs (AAFL, imp8/4), front view (3D model)

The purple area is the result of the intersection of 16 out of 19 located areas, it confidently covers the sensor that served as a calibrator.

Here is a view of the other half of the sphere:

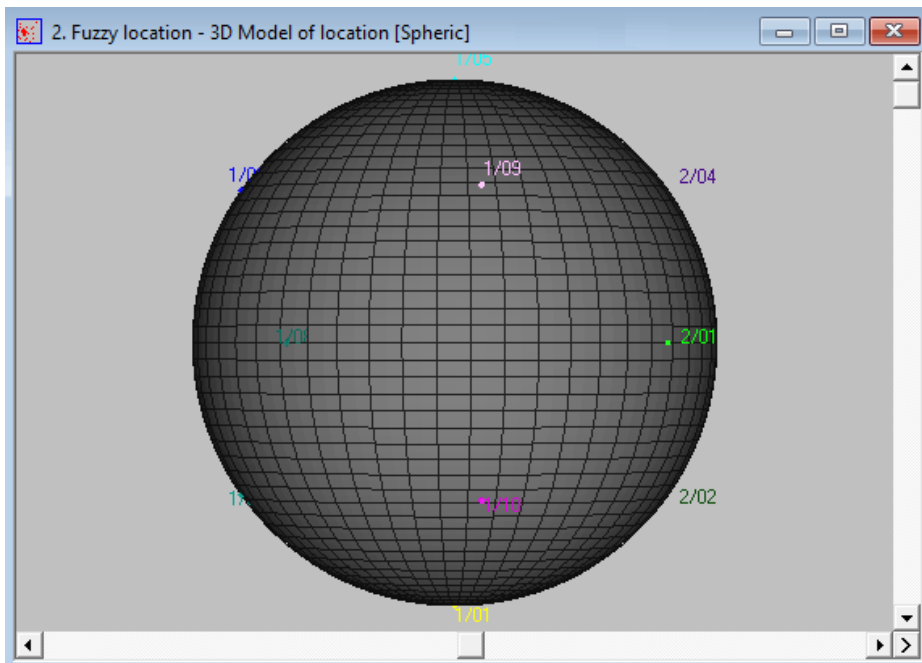


Fig. 4.7. Fuzzy location by packs (AAFL, imp8/4), rear view (3D model)

These three slightly overlapping yellow areas are most likely random. This is easy to verify.

Since the data is clearly good, we will choose packs with at least 10 impulses for location and will locate 6 at a time. Here is the result:

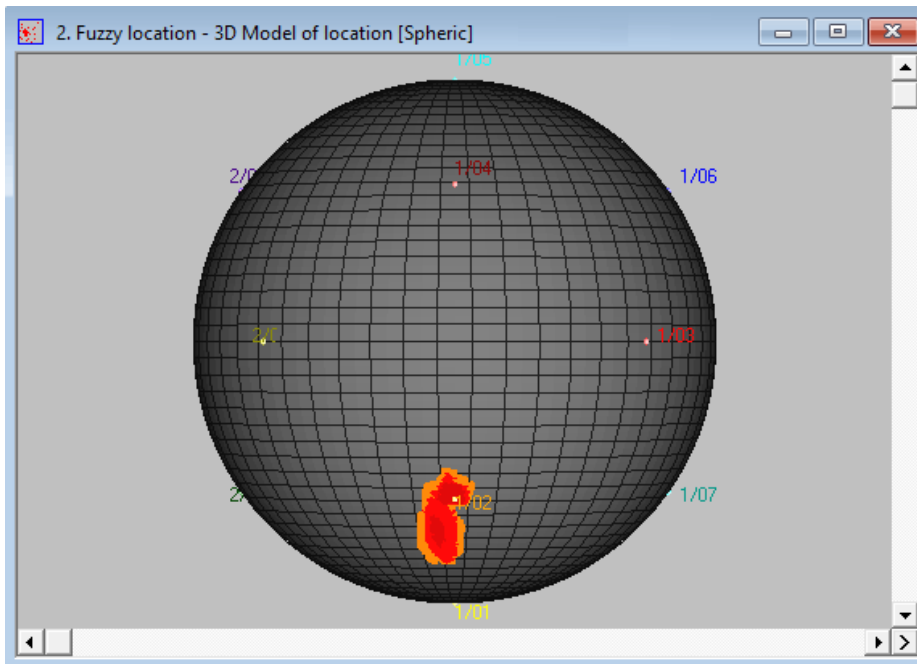


Fig. 4.8. Fuzzy location by packs (AAFL, imp10/6), front view (3D model)

The purple section is still the intersection of the 16 located areas, but it is smaller, since the location is more accurate using 6 sensors. In this case, there are no more false regions at all, three regions on the reverse side of the sphere have disappeared. Finally, after making sure that the source is located correctly, you can try to locate it even more accurately by locating 8 impulses (and selecting packs of at least 12 impulses).

The final result is:

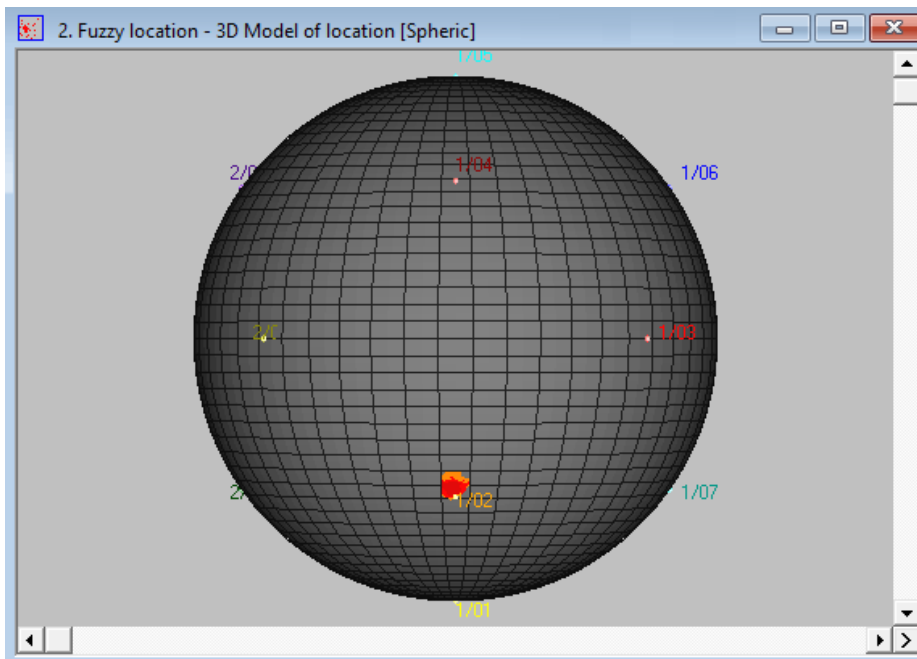


Fig. 4.9. Fuzzy location by packs (AAFL, imp12/8), front view (3D model)

We see that the purple area has become even smaller, and although now it is already the result of the intersection of only 7 location areas, it is obviously obtained from the most informative packs containing data from all 12 sensors used for location. The color of the area

has not changed, since the clustering option was chosen by the percentage of the number of events in the cluster from the accumulated maximum: both 16 out of 19 areas, and 16 out of 16, and, in the last example, 7 out of 7 correspond to the last interval: more than 80%.



Chapter 5. Calibration procedure



Chapter “*Calibration procedure*” is entirely devoted to the calibration procedure.

5.1. Channel calibration

Used abbreviations and terms

- ◇ The following abbreviations are used in the text:
 - ATI is difference in AE pack impulse arrival times.
- ◇ The following terms are used in the text:
 - AE pack is a set of AE impulses received by different channels and emitted by single AE event.
 - Calibration pack is a pack that is formed during the operation of the calibrator, the first AE impulse of which is the reference one, from which the time for calculating the ATI for the remaining impulses of the pack is counted.

When emitted by the module, the AE reference impulse is marked with zero amplitude and unit duration. When an external simulator is operating, the reference impulse arrives at the channel, the sensor of which is closer to the calibrator.
 - Pack duration is a value determined by the ratio of the largest distance between the sensors installed on the testing object and the minimal velocity of the AE impulse.

When a wave propagates through oil, the velocity is 1100...1200 m/s, through water - 1300...1400 m/s, for steel structures - 2800...3200 m/s. When setting the value of the minimal velocity, it is recommended to set it as 80 % of the real one in order to set some margin for the pack duration.

Calibration overview

Calibration will be understood hereinafter as the procedure for checking the quality of the sensor installation at the testing object.

- ◇ This procedure has three interacting parts:
 - repeated and successive emission of an elastic wave by sensor connected to the modules of complexes of type **A-Line DDM**;
 - registration by the equipment of AE impulses, which are the front of the emitted wave, and calculation of their parameters;
 - using a special algorithm in the system software to analyze the obtained parameters of AE impulses and obtain an assessment of the quality of such a "sounding".
- ◇ In addition to emission by the **A-Line DDM** type module, **manual** emission is allowed (at a distance of 10...15 cm from each module on testing object according to the standard technique). With manual emission, it is allowed to use a Hsu-Nielsen source or any other source that provides the generation of series of elastic waves and leads to the registration of these waves by at least a pair of sensors. The procedure assumes the same settings and composition of all channels used in the calibration (including sensors). In order to take into

account the complexity of the acoustic situation at the testing object and correctly calculate the parameters of the recorded elastic waves, the general calibration procedure provides for two preliminary tests for software adjustment of the equipment parameters:

- in the first test, a per-channel estimate of the background noise level at the testing object without loading is performed (without any emission), a priori assuming the equality of these levels for different channels;
- in the second test, all channels are tested in turn and the fact of their reception is revealed.

After the completion of each test, the characteristics of the complex are assigned, in which the calculation of the parameters of the received calibration impulses will be the best.

- ◇ When channels are identified that are out of the overall statistics by more than the specified value, the operator must choose one of three actions (Fig. 5.6):
 - abort procedure;
 - exclude the channel and continue the procedure;
 - reinstall the sensor, assuming that the situation is caused by poor-quality installation of this sensor on the testing object, and after reinstallation, restart the procedure.
- ◇ The calibration procedure is considered successful only if both tests and the calibration itself are successfully completed. If the operator interrupts the procedure at any stage, then the calibration is considered "failed". Other possible sources of calibration failure could be:
 - difficult acoustic environment actually prevailing at the testing object;
 - cases of a satisfactory acoustic situation at the testing object that were not taken into account when pre-setting the calibration parameters.

Information about each step of the calibration procedure can be shown by sound signals, displayed in the main time windows by text labels, and also on location pictures by filled colored areas.

General settings

All settings of the calibration procedure are stored in a file with the extension ***.clb**. In order to load ready-made settings, in the main menu **Location** select the sub-item **Open calibration**, and to create a new settings — **New calibration**. As a result, the dialog box **Calibration options**.

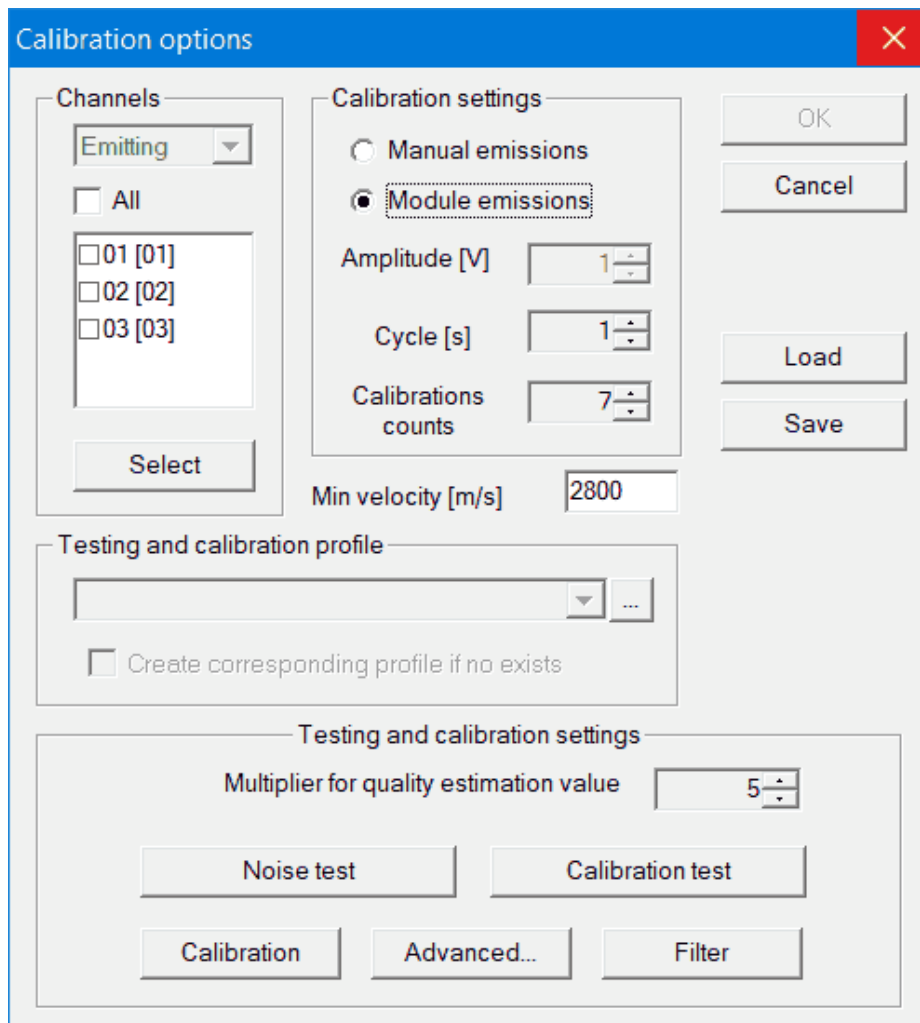



Fig. 5.1. Dialog box **Calibration options**

In this dialog box, make all the necessary settings.

- ◇ In the **Channels** group, select the channels (at least 2) that will take part in the calibration. For this:
 - Press the button **Select**, which activates the standard dialog **Select channels**. After selecting the channels, a list will be filled in, in which it is necessary to specify those numbers that will take part in the emission (in the case of manual calibration, for each selected channel, it is necessary to simulate an external source according to the standard method);
 - Select the switch **All** to emit all channels selected for calibration.

Until at least two channels are selected for emission, the **OK** button will not be available to complete the setup.
- ◇ In the **Calibration settings** group, set the emission parameters:
 - Select the type of emission, **Manual emissions** or **Module emissions**. If you choose the second option, it will be possible to select the interval between emissions in seconds, and after setting **New measurements**, changing the amplitude value will become available (spinner **Amplitude [V]**), supplied by the module to the sensor for emission. Permissible amplitude change range — 10...140 V.
 - Set the number of emissions in the list **Calibrations counts**. The minimum value is 7. For the **Manual emissions** case, only the first of them will be included in the statistics.

- ◇ The **Min velocity** parameter takes part in the time selection of received data. Recommendations for setting this parameter are given in Chapter 2 when describing the term "pack".
- ◇ The program has the ability to store the hardware settings in the profile selected for this during calibration. To enable this feature, do the following:
 - in the group **Testing and calibration profile** click on the button  ;
 - select an existing hardware profile from the list.
- ◇ To define a new calibration profile based on the current one, do the following:
 - in the list box, enter a new name for the profile;
 - activate the switch **Create corresponding profile if no exists**.

After closing the dialog **Calibration options** a new hardware profile will be created.

The calibration profile becomes current at the start of calibration, and after it is completed, the previous profile becomes current. If the profile field has not been selected, then the current profile will be used for tests and calibration. During the calibration, it is not allowed to change the settings, so the following will not be available: dialogs for configuring channel parameters and a dialog for configuring equipment profiles; selection of the current profile; starting a channel for emission by double-clicking on the color display area of the channel on **View Bar** (see menu **View – View Bar**).

- ◇ All calculations in the calibration procedure are performed in normalized values, which are in the range 0...1. To specify a different normalization, specify in the group **Testing and calibration settings** in the field **Multiplier for quality estimation value** required value in the range 1...1000.
- ◇ To activate the dialog **Advanced calibration options** shown in fig. 5.2, press the **Advanced...** button in the **Testing and calibration settings** group of the **Calibration options** dialog box.

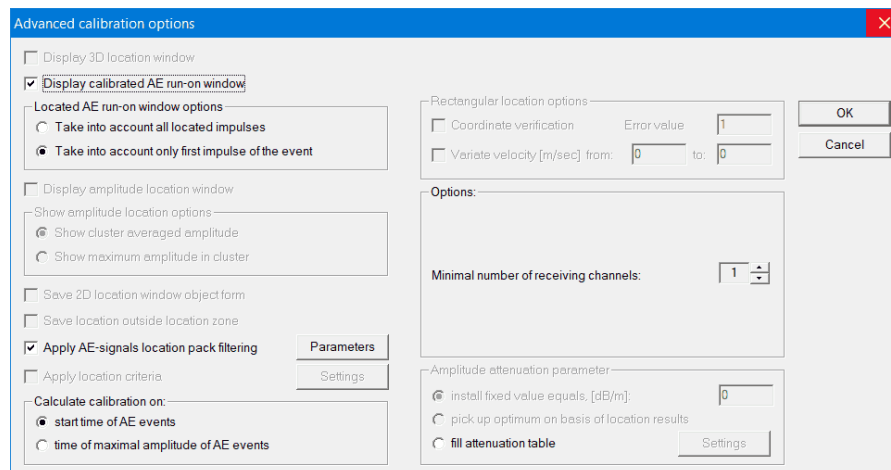


Fig. 5.2. Dialog box **Advanced calibration options**

- ◇ To display the accumulation of calibration packs, activate the item **Display calibrated AE run-on window**.
- ◇ Group **Calculate calibration on** (fig. 5.2) allows make an appropriate choice between the items **start time of AE events** and **time of maximal amplitude of AE events**. Select the first item to use in the calculation of the difference between the emission time and the arrival time of AE impulses as the moment of crossing the threshold level.

- ◇ Set in the group **Options** (fig. 5.2) in the paragraph **Minimal number of receiving channels** number of corresponding channels. For manual calibration, this value is at least 2 (at least two receivers), and for modular calibration it is at least 1 (one receiver, and the emitter does not count).
- ◇ Activate the dialog **Parameters of AE-pulses pack** (fig.5.3) by pressing the button **Parameters** of the group **Apply AE-signals location pack filtering** (fig.5.2).

Fig. 5.3. Dialog box **Parameters of AE-pulses pack**

- ◇ In the **Pack selecting parameters** group, set the item **Maximum distance between channels, [mm]**.

It has already been mentioned above, when describing the item about the minimal velocity. The value of this offset refers to a group of channels in which the emission from each sensor will form a calibration pack with a duration calculated from the given values.

To save the assigned calibration parameters in a file, use the **Save** button (Fig. 5.1), to download, use the item **Open calibration** of the menu **Location** or in the dialog **Calibration options** press the button **Load**. After pressing the **OK** button in the calibration settings dialog (Fig. 5.1) on the current tab the main information window **Channel calibration** will be displayed.

Setting up a noise level test

To provide access to the test in the dialog **Calibration options** in the group **Testing and calibration settings** (Fig. 5.1) press the button **Noise test** to activate the **Noise level testing parameters** dialog noise level test (Fig. 5.4), in which set the switch **Turn ON test**.

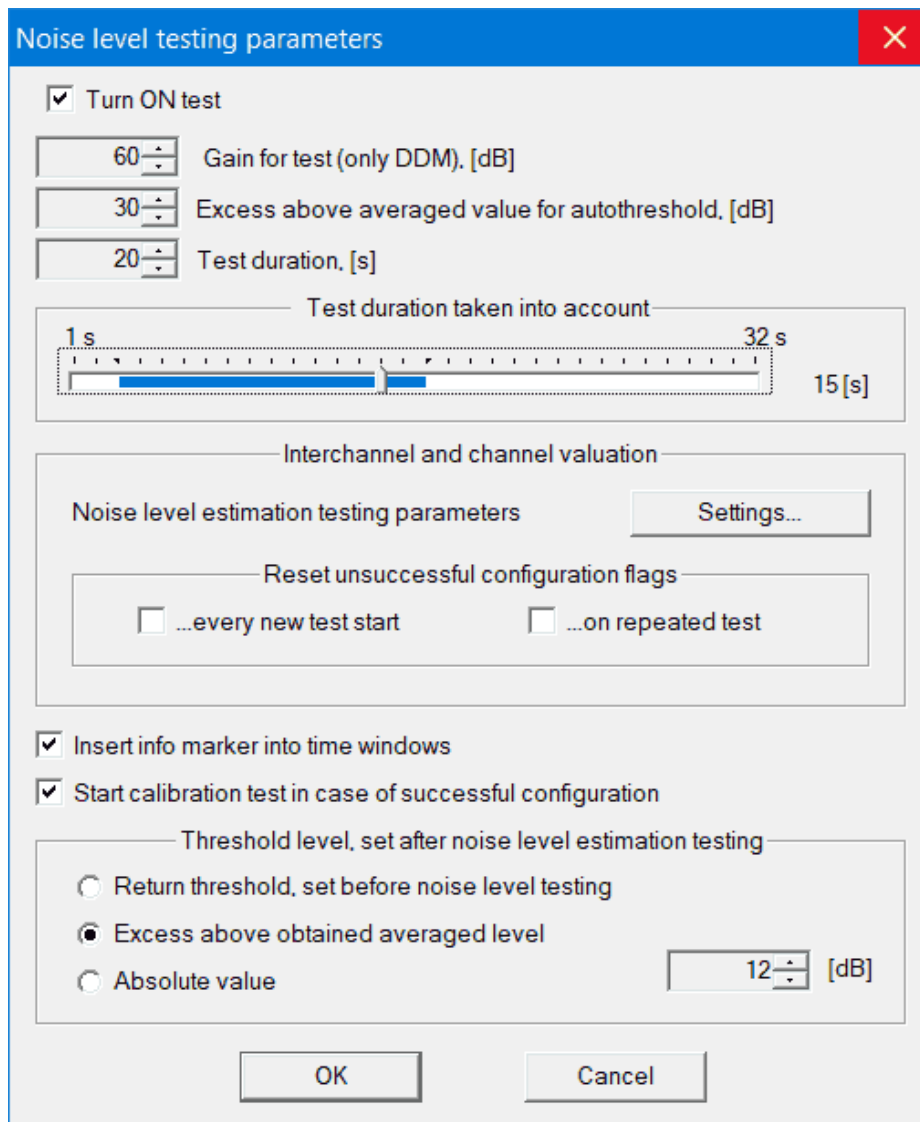


Fig. 5.4. Dialog box **Noise level testing parameters**

During the specified test duration (Fig. 5.4), per-channel, per-second noise level values are recorded. This data is used to identify those channels in which the noise level stands out from the overall behavior statistics. If such channels are found, then the operator in the dialog (Fig. 5.6) must choose one of the three further actions described in Chapter 3. Channel dropout is determined by the average value of the noise level, from which the threshold for further measurements can be detuned.

Set the noise level test parameters in the **Noise level testing parameters** dialog box (Fig. 5.4).

◇ Using the appropriate spinners set:

- Value of **Gain for test (only DDM), [dB]** parameter, which can be set only for **A-Line DDM** complexes. Set to 60 dB for more accurate noise level recording.
- The value of the parameter **Excess above averaged value for autothreshold, [dB]** in the region of 20...40 dB to ensure greater reliability test.

- The value of the **Test duration** parameter, which cannot be less than 7 seconds so that the statistics are not inconsistent. Set this value in the range of 10...20 seconds with insignificant self-noise on testing object and more than 20 seconds for **noisy** test object.
- ◇ In the **Test duration taken into account** group, use the horizontal slider to set the appropriate time, which is limited from above to 32 seconds. It is recommended to set it to the maximum, but less than the duration of the test by 2...3 seconds. During the duration of the noise test, only the final time specified in the scoring duration will be used for calculations.
- ◇ Select the radio button **Insert info marker into time windows** to fix the test history in time windows with a vertical dotted line with a marker (Fig. 5.4).
- ◇ Deselect the **Start calibration test in case of successful configuration** radio button (fig. 5.4) in order to use this test as an independent procedure to set the threshold level from the calculated average, and make sure that the profile for the test is not set in the dialog (Fig. 5.1). Set the selection if the results of this test require you to run a calibration test.
- ◇ The group **Threshold level, set after noise level estimation testing** contains the following elements:
 - **Return threshold, set before noise level testing**, the choice of which is justified in case of refusal to autostart the calibration test when starting after a new measurement .
 - **Excess above obtained averaged level**, the choice of which, together with setting the excess value in the range of 12...30 dB, is justified when autostart of the calibration test is set.
 - **Absolute value**, may be preferred for testing object with constant noise level.

Let's take a closer look at the grades used in the test:

- ◇ In the **Interchannel and channel valuation** group (fig. 5.4) click on the button **Settings...** to activate the dialog **Noise level testing estimation parameters** (Fig. 5.5).

Fig. 5.5. Dialog box **Noise level testing estimation parameters**

- ◇ The following group elements are used in this dialog box:
- Elements of groups **ASL control...** and **STD control** responsible for per-channel ratings.
 - Elements of groups **(ASL)** (average value) and **(STD)** (standard deviation) are statistics that are used during the test to estimate the average value of the noise level (**Noise amplitude**) for the period (**Average time**). The **STD** value indicates the spread of the estimated value.

After the expiration of time equal to **test duration** (Fig. 5.4) comparison of the calculated values and the introduced restrictions. If at least one of the specified limits for the **ASL** values is not met, then the message **Suspicious signal level obtained on channel ###** will be displayed in the dialog asking for further action (Fig. 5.6); if at least one of the specified limits for the **STD** values is not met, then the message will begin with the words **Instability of the signal level ### has been detected**. This dialog is described in Chapter 3.

Removing a channel results in a setup failure flag being set. This flag can be "cleared" only in two cases: when repeating (restarting after pressing the **No** button in the dialog (Fig. 5.6) of the test after pressing the button **No** in the dialog (Fig. 5.6) and at a new start of the test from the calibration panel. For each such case, you must set the appropriate switch in the group **Reset unsuccessful configuration flags** in the dialog (Fig. 5.4):

- ◇ The first constraint (Fig. 5.5) is the minimum value.

For **STD** this value is limited from below 0.3 dB, and for **ASL** -15 dB. The recommended value for **STD** is 0.5 dB, for **ASL** — 20...25 dB, moreover, for **ASL** it is better to set it experimentally (for **sensor** with a built-in **preamplifier** this is impossible). If the condition is met under which the level **ASL** is less than the specified minimum, then in the dialog with the request a warning will be issued that a situation with a short circuit of the measuring circuit is likely (Fig. 5.6).

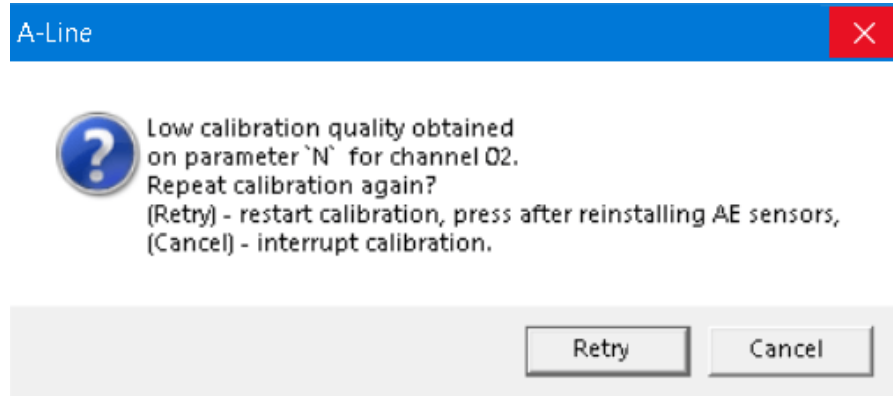


Fig. 5.6. Per-channel test confirmation dialog

- ◇ The second constraint is the maximum value, or upper constraint. It allows you to track the situation with sensor self-excitation (when the "ground" braid breaks), at which the level of **ASL** increases sharply, and situation with a large range at the same level of the measured value. By default, this value for **ASL** is 30 dB, and for **STD** - 3 dB.
- ◇ The third value set in the dialog serves to limit from above the deviations of the measured value from the calculated average. The default value for **ASL** is 6 dB, and for **STD** 2 dB.

Setting up a calibration test

This test is only available for **A-Line DDM** complexes. Pressing the button **Calibration test** (Fig. 5.1) opens the dialog **Calibration test parameters** (Fig. 5.7). To activate access to the test, select the field **Turn ON**. After that, the main test settings will become available:

Fig. 5.7. Dialog box **Calibration test parameters**

The purpose of this test is to detect the absence of calibration packs from emission. It is strongly recommended that during the first test of calibration on testing object or even before the test, choose a gain that will not cause the ADC overload to be observed, otherwise the amplitude and energy values will not correspond to reality.

- ◇ Group **Gain for test and calibration period (only for DDM)** contains a three-position switch:
 - **Gain, set before testing**, the choice of which is justified when using the gain specified in the equipment settings.
 - **Constant gain** allows you to set a specific gain value for the duration of the test and the calibration itself.
 - **Decrease automatically in case of amplitude overflow** (not available yet).
- ◇ The group **Threshold level for test and calibration period** contains a two-position radio button:

- **Threshold, set before testing**, the choice of which is justified if the noise level test was applied before the calibration test, with which the optimal threshold level value.
 - **Absolute value** which makes sense if you set a specific threshold level for the test and the calibration itself.
- ◇ In the field **Number of radiation acts on every channel**, enter the appropriate value (it is limited from below by the number 3). The upper limit is equal to the number of emissions of the main calibration procedure, (Fig. 5.1). If no incoming calibration packs were registered from emission by one channel (the minimum number of receiving channels in the calibration pack is set in the dialog in Fig. 5.2), then the operator a dialog will be displayed with a request (Fig. 5.6), but with a warning **When setting up the calibration, it was detected that there was no reception of impulses from channel emission # ##**. Three buttons will also be available in the dialog: **Yes**, **No** and **Cancel**, the meaning of which remains the same as before.
- ◇ Group **Reset unsuccessful configuration flags** contains the same switches as in the noise level test, and their purpose is the same: on a new start and on a repeat, start test **from scratch** or remember previous failed settings. It is important to clarify that these flags are individual for each test and for each channel. It is possible to reset all flags at the same time only when updating the calibration, when the dialog is called (Fig. 5.1), after which it is necessary to close the dialog with the button **OK**.

Switches **Insert info marker into time windows** and **Start general calibration in case of successful configuration** have the same meaning as for the noise level test, except that the calibration itself can be run after the test.

Settings and calibration algorithm

To open the dialog **Calibration settings**, click the button **Calibration** in the dialog **Calibration options** (Fig. 5.1). The dialog contains a switch **Insert calibration marker into time windows**, the meaning of which was clarified in the sections on noise and calibration tests.

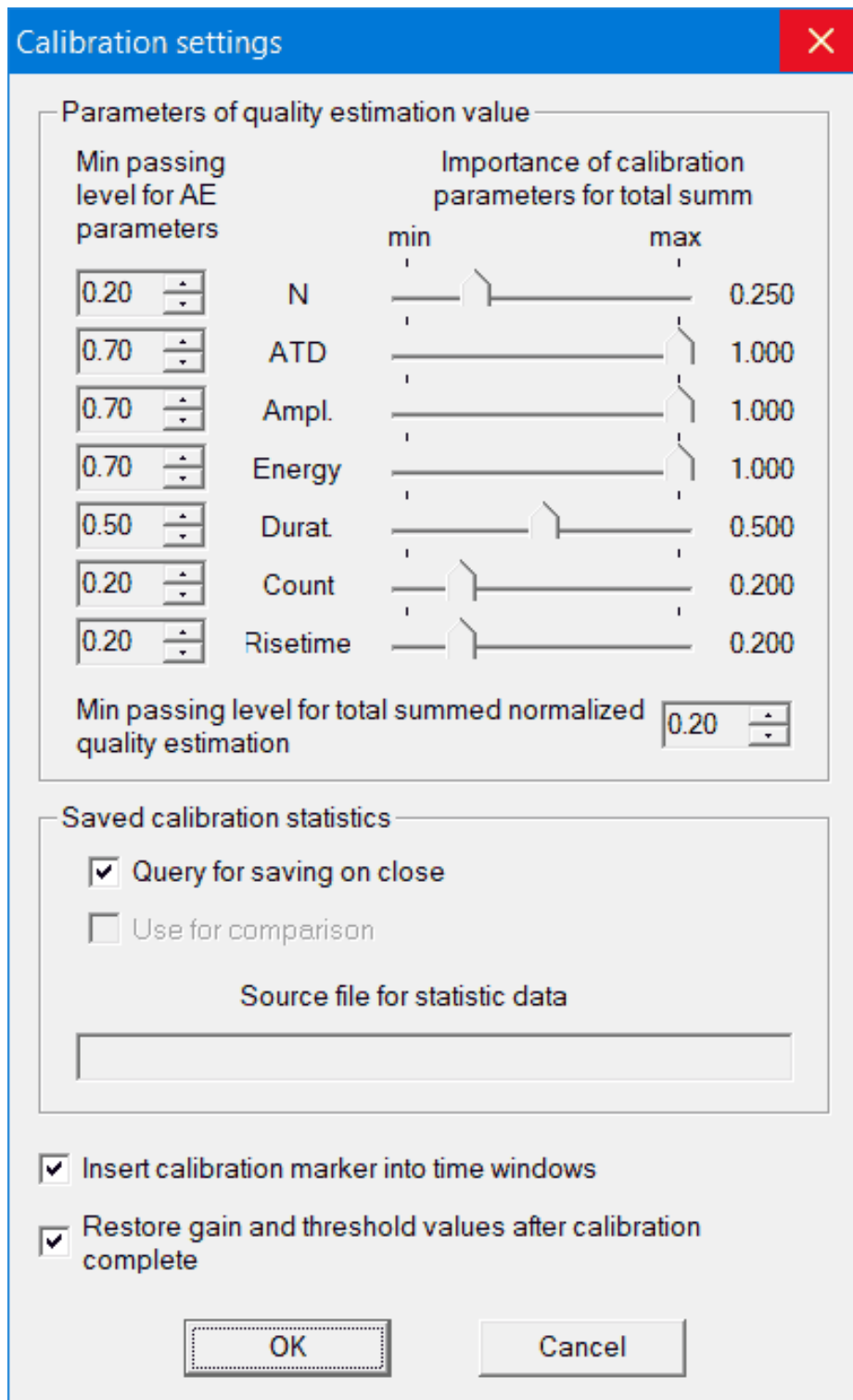


Fig. 5.8. Dialog box **Calibration settings**

- ◇ Select the switch **Restore gain and threshold values after calibration complete**, if a calibration profile has not been specifically set in the dialog in Fig.5.1.
- ◇ Group **Parameters of quality estimation value** contains the values of the minimum passing levels normalized to unity according to the registered AE impulse parameters and their significance in the total amount. This means that an individual score for each parameter is used to calculate the quality of the calibration, taken with a given weighted multiplier:

$$Q = \sum_{p=1}^n M_p \cdot Q_p \quad (1),$$

where:

Q is overall score based on calibration results;

M is number of analyzed AE impulse parameters;

Qp is evaluation value by the calibration parameter;

Ap is a weighted significance value for the calibration parameter p, such that: $pMAp=1$ (2).

- ◇ Let's consider the algorithm for obtaining Qp, estimates for each AE impulse parameter. Among the studied parameters, as can be seen from Fig. 5.8, available:
 - N is number of received/emitted AE impulses;
 - ATI is difference between emitted and registered AE impulses;
 - A is maximal amplitude;
 - E is energy;
 - Dur is duration;
 - Count is number of AE packs;
 - RT is rise time.
- ◇ All statistics are displayed in the table of the window **Channel calibration**. The **Stat. char's** group contains a switch for displaying the following statistical characteristics: mean, median value, and variation in percentage terms.

Summary	N	ATI, ms	A, dB	E, dB	Dur, μs	Count	RT, μs
Stat. char's	chan	-> 01	-> 02				
Mean	01 (!)->	[2]	.				
Median	02 (!)->	+	[7]				
Var %	qual.	5.0	...				

Fig. 5.9. Dialog box **Channel calibration**

- The choice of **Median** is set by default and is justified in terms of minimizing the impact of outliers in the sample statistics.
- To display statistics by variation, select the radio button **Var %**. The variation will allow you to judge the statistical dispersion of the sample, numerically equal to the percentage of the standard deviation to the arithmetic mean.
- To display the average value, select the mentioned position switch **Mean**.
- ◇ Use the bookmarks panel to toggle the display according to the relevant parameters (Fig. 5.9). The **Summary** tab contains the median quality scores **Qmean** for each parameter listed above **p** and for each receiving channel **c**.
- ◇ For other tabs, below the square matrix of statistics, there is a quality line for the selected statistical characteristic. As can be seen from the headings of the headings of the table of statistics, the rows correspond to the emitting channel (symbol (!)->), and the columns correspond to the receiving channels (symbol ->).
- ◇ Parameters **N** and **ATI** are calculated based on the results of compiling **calibration pack**. Statistics is according to **N**, the number of received / emitted impulses, is compiled as follows: the number of calibration packs when emitting a certain channel is written in a square

matrix in a diagonal element in parentheses (...), in the column and line corresponding to the channel number (Fig. 5.9). Statistics on received **AE impulses** is displayed in the remaining cells of the table - dots, pluses, numbers in brackets or without. Thus, if the number of received **AE impulses** for the receiving channel is less than four, then a dot is displayed. If the number of received is equal to or one less than the number of emissions, then a plus is displayed. If the number of received **AE impulses** is 1.5 times less than the number of emitted ones, then this number is displayed in "reverse" angle brackets (for example, $\langle 4 \rangle$ for 8 emitted), otherwise without them.

- ◇ An undefined quality value in the corresponding cell of the table is indicated by a period symbol — «.» (see for channel 1/01 in Fig. 5.9). Therefore, in order to obtain calibration quality values, it is necessary to register at least four calibration packs for the two minimum channels in the calibration. For channels 1/02 ... 1/04, the quality is «**5.0**», which means that the number of received impulses and emitted **AE impulses** are equal channel 1/01.
- ◇ Let's consider getting statistics for **ATI**. In the case of **A-Line DDM** complexes, **calibration pack** is triggered by a emission impulse. In the window of synchronous text viewing of AE impulses, the parameters of the emission impulse differ from ordinary impulses. The **Time** parameter displays the emission time, which is ten microseconds less than the time when the acoustic wave is generated under the sensor, which is due to the **sensor** inertia. The **Duration [µs]** parameter has a single value, and the rest s are zero. For uniform display in the statistics window, it is considered that the duration is also zero.
- ◇ For the **A-Line PCI** complex, the triggering impulse will be the one received by the nearest **sensor** from a emitting external source, so there will be no zeros in the **AE impulses** parameter tabs brackets on the main diagonal of the matrix. **ATI** is calculated as the difference between the times of received and triggering impulses. It is this statistic that is the main one for the auto-arrangement procedure, where the determining factor is the time spent by **AE impulses** to overcome the distance from the trigger to all receiving channels. On Fig. 5.10 displays median statistics for **ATI** for a group of four sensors located on plate with a maximum distance of the first from the fourth by 30 cm.

Summary	N	ATI, ms	A, dB	E, dB	Dur, µs	Count	RT, µs
chan		-> 01		-> 02			
01 (!)->		(0)		0.083			
02 (!)->		0.086		(0)			
qual.		5.0		5.0			

Fig. 5.10. Page **ATI** after calibration

- ◇ The quality of **ATI** calibration can be estimated at a slightly above average level, since the results are displayed on a five-point scale. For calibration (Fig. 5.10), the variation statistics looks like this:

chan	> 01	> 02
01 (I)->	(0)	+
02 (I)->	+	(0)
qual.	5.0	5.0

Fig. 5.11. Page **Variation** of dialog box **Channel calibration**

As you can see from Fig. 5.11, the variation is minimal when emitting channel 1/04, when the pluses in the cells indicate a small amount of variation. At the same time, for different parameters, pluses are put down for different lower threshold values of the variation **var l**: for **ATI**, amplitude and energy — **var l** = 2 %, for duration, overshoot and rise time parameters — **var l** = 7 %. Values displayed in back curly brackets exceed the upper threshold value for variation **var u** and for **ATI**, amplitude and energy **var u** = 6 %, and **var u** = 20 %.

- ◇ After calculating the quality value for various parameters **AE impulses**, a comparison is made with those specified in the **Calibration settings** dialog (Fig. 5.8) values from the group **Min passing level for AE parameters**. If the channel quality is less than the specified one, then a query dialog is displayed (Fig. 5.6) with the message **Suspicious signal level obtained on channel ###** for subsequent possible restart after reinstallation of **sensor**.

In case of a successful assessment by the parameters **AE impulses**, the final value of **Q**, calculated by formula (1), is compared with the value of the minimum passing level according to the overall total normalized quality assessment, assigned in the dialog **Calibration settings** (Fig. 5.8).

Running tests and calibrations

After making the necessary settings for the tests and the calibration itself, described in 11.3-11.6, and closing the **Calibration options** dialog (Fig. 5.1), on the current tab, the window **Channel calibration** will be displayed (Fig. 5.10).

- ◇ In the statistics table, before starting a new measurement or reading a file, the following will be displayed:
 - empty cells for the values of the test statistics and the calibration itself;
 - symbols "..." for quality ratings;
 - zeros for the noise level test.
- ◇ Switching between tests and calibration is done only with the mouse on the calibration panel:

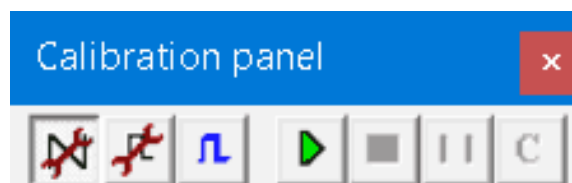


Fig. 5.12. Calibration Panel

The first button on the left allows you to select a test by noise level, the second selection of a calibration test, the third selection of the calibration itself. Button with a green triangle (seventh button from left) start test/calibration, eighth stop test/calibration, ninth suspend, tenth resume after suspend.

- ◇ Buttons for starting tests will be available only after the start of the complex, and the button for starting calibration is available immediately after starting the program.
- ◇ In order to obtain calibration statistics from the data recorded in the file, do the following:
 - upload data file;
 - load calibration settings;
 - select calibration mode (third button on the calibration panel);
 - click start calibration button.
- ◇ In the calibration setup file for the noise level test, you can save the current running state. This can be useful if a complete calibration cycle must be carried out immediately after the start of a new measurement and the start of the complex. In the calibration settings for this case, check the boxes:
 - **Start calibration test in case of successful configuration** in the dialog (Fig. 5.4).
 - **Start general calibration in case of successful configuration** in the dialog (Fig. 5.7).
- ◇ To save the running state of the noise level test, do the following:
 - start the complex to receive data;
 - select the noise adjustment mode;
 - click start test calibration button;
 - click the data acquisition stop button (without clicking on the calibration test stop);
 - select the item **Edit current calibration** in the main menu and from the dialog **Calibration options** (Fig. 5.1), save the calibration settings.
- ◇ In order to obtain calibration statistics from the data recorded in the file, do the following:
 - upload data file;
 - load calibration settings;
 - select calibration mode (third button on the calibration panel);
 - click start calibration button.
- ◇ In the calibration setup file for the noise level test, you can save the current running state. This can be useful if a full calibration cycle is to be carried out immediately after starting a new measurement and starting the system. In the calibration settings for this case, check the boxes:
 - **Start calibration test in case of successful configuration** in the dialog (fig.5.4);
 - **Start general calibration in case of successful configuration** in the dialog (fig.5.7).
- ◇ To save the running state of the noise level test, do the following:
 - start the system to receive data;
 - select the noise adjustment mode;
 - click start test calibration button;
 - click the data acquisition stop button (without clicking on the calibration test stop);
 - select the item **Calibration settings** in the main menu and from the dialog **Calibration settings** (Fig. 5.1), save the calibration settings.

- ◇ To start the calibration automatically (the calibration settings file must contain the saved running state of the noise level test), the operator has two options:
 - run the program from the command line, which contains the path to the calibration settings file (you can use the // key to specify the directory of settings files);
 - stop data collection, load calibration settings, and then start data collection.
- ◇ After running the noise level test, statistics will be updated every second in the table of the window **Channel calibration**.

chan	01	02	Mean	Nsigma
ASL, dB	28.70	28.51	28.61	1.00
qual.	3.74	3.78		
STD, dB	0.81	0.30	0.56	1.00
qual.	5.00	5.00		
Sum.		

Fig. 5.13. Test statistics by signal level

- ◇ After running the noise level test, statistics will be updated every second in the table of the window **Channel calibration**.

chan	01	02	Mean	Nsigma
ASL, dB	28.70	28.51	28.61	1.00
qual.	3.74	3.78		
STD, dB	0.81	0.30	0.56	1.00
qual.	5.00	5.00		
Sum.		

Fig. 5.14. Test statistics by signal level

- ◇ According to the results of the test, either a message will be displayed about unsuccessful tuning on any channel, or (if successful), a calibration test will be started with autorun specified in the settings.
 - If this flag was cleared, then the stage will be completed at this stage and to proceed to the calibration test, you must manually select the appropriate button on the calibration panel and press the test start button.
 - If the calibration is forced to start without passing the tests successfully, the system will issue a warning **Calibration setup (test) was not completed successfully. Are you sure you want to start calibration?**

The same buttons **Yes**, **No** and **Cancel** will be available in the dialog. Pressing the first button starts the calibration, pressing the second button starts the calibration test, pressing the **Cancel** button performs the corresponding action.



Section 2

A-Line OSC

Chapter 6. Wavelet analysis of AE impulses in thin-walled objects



The “*Wavelet analysis of AE impulses in thin-walled objects*” chapter describes and substantiates the use of continuous wavelet transform for the analysis of acoustic emission signals in thin-walled objects: visualization and mode separation, determination of the distance to the source of acoustic emission by one waveform, noise filtering, refinement of the signal arrival time. Appropriate techniques are built into the A-Line OSC software.

6.1. Guided waves

One of the main goals of new developments in the field of acoustic emission (AE) is to increase the accuracy of determining the coordinates of AE sources.

In 90% of cases, AE testing is carried out on thin-walled objects with a wall thickness of 3 - 100 mm. This value is comparable to the acoustic wavelengths, which at typical operating frequencies of acoustic emission sensors of 30 - 500 kHz lie in the range from 5 to 170 mm. In this situation, the pattern of propagation of acoustic oscillations changes significantly compared to the simplest case of an infinite volume or half-space, and therefore it becomes impossible to use simple models suitable for massive objects based on volumetric longitudinal, transverse, and Rayleigh waves. There is a need to use the model of guided waves. Such waves are distinguished by strong dispersion - the presence of a dependence of the propagation velocity on frequency. Therefore, despite the fact that the AE impulse is emitted by a microcrack in the form of a pulse with a duration of 0.001 - 0.01 μs , various frequency components of the signal arrive at the acoustic emission sensor with a spread of tens and hundreds of microseconds, which significantly reduces the accuracy of source location.

The simplest and at the same time the most famous case of normal waves is the Lamb waves propagating in flat sheets (Fig. 6.1). This model can also be used in the case when the testing object is made up of sheets, the radius of curvature of which is large compared to the thickness, for example, for a tank filled with gas.

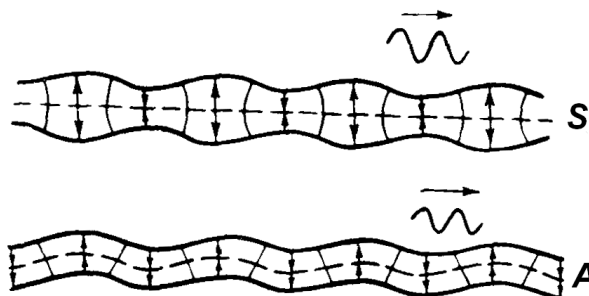


Fig. 6.1. Normal waves in plates

The solutions of the wave equation in the plate depend on the frequency, and there can be several solutions at the same frequency. Each such solution, called a mode, has its own pattern of oscillations in the plate, as well as its own propagation velocity (Fig. 6.2). In the case of Lamb waves, it is convenient to divide all modes into symmetric S_n and antisymmetric

A_n , depending on the corresponding oscillation patterns. The total number of possible modes at a given frequency increases with the oscillation frequency. As a rule, not a single mode propagates in the plate, but a linear combination of modes of different orders, while the main part of the energy is transferred by the zero modes A_0 and S_0 .

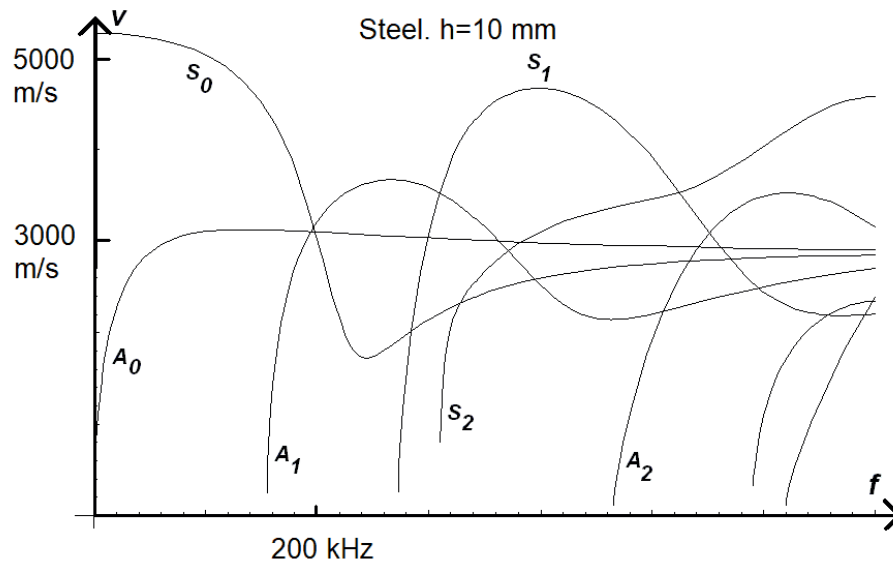


Fig. 6.2. Frequency dependences of the group velocity of Lamb waves

In the limit at $f \rightarrow \infty$, the group velocities of all modes tend to the Rayleigh surface wave velocity, for steel ($C_L = 5900$ m/s, $C_T = 3100$ m/s) equal to 2900 m/s. In the limit as $f \rightarrow 0$, the group velocity of the zero antisymmetric mode tends to zero as

$$C_{A_0}(f \rightarrow 0) = 2 \cdot \sqrt[4]{\frac{E}{3\rho(1-\mu^2)}} \sqrt{\pi f h}, \text{ while the group the velocity of the zero symmetric}$$

mode tends to $C_{S_0}(f \rightarrow 0) = \sqrt{\frac{E}{\rho(1-\mu^2)}} = C_T \sqrt{\frac{2}{1-\mu}}$ [2], which is 5300 m/s for steel. Here

h is the plate thickness, E is Young's modulus, μ is Poisson's ratio, ρ is the material density, C_L and C_T are the velocities of volumetric longitudinal and transverse waves in the material of the object. There is a characteristic frequency at which the velocities of all three modes A_0 , S_0 and A_1 are equal. For steel, it is approximately equal to $2 \text{ MHz} \cdot \text{mm}/h$, where the plate thickness h is given in mm.

The second common case is pipelines (Fig. 6.3), where wave propagation is described by the Pochhammer-Chree theory [1-6]. In this case, the modes are divided into 3 classes: T_{mn} -modes (torsional), F_{mn} -modes (bending) and L_{mn} -modes (longitudinal). Except when the pipe diameter and wall thickness are comparable, the frequency dependences are almost identical to those for Lamb waves (Fig. 6.4). In particular, there is also a characteristic frequency in the region of $2000 \text{ kHz} \cdot \text{mm}/h$, near which the graphs of the frequency dependence of a number of lower-order modes intersect. A significant difference takes place only near the second characteristic frequency, for steel approximately equal to $2000 \text{ kHz} \cdot \text{mm}/D$, where D is the pipe diameter, given in mm. However, this has practically no effect on work in the field of AE, since the second characteristic frequency, as a rule, is in the lower edge of the operating frequency range of AE equipment - in the region of $10 - 30 \text{ kHz}$.

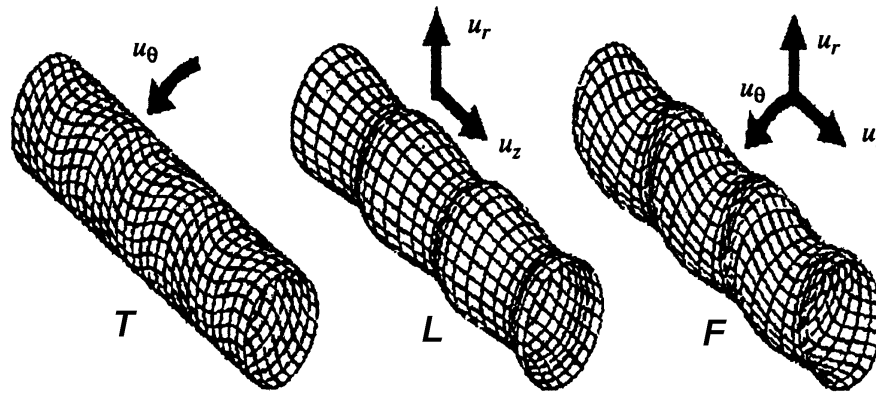


Fig. 6.3. Guided waves in pipes [6]

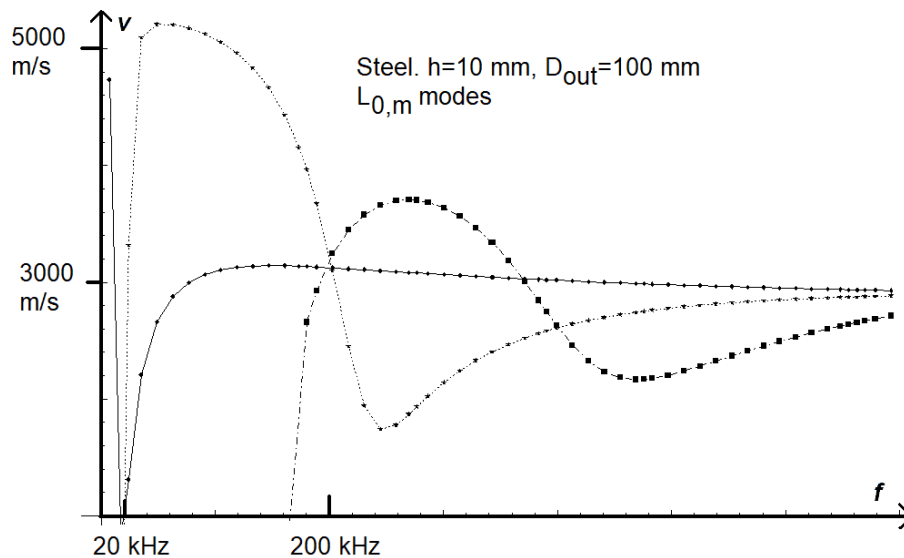


Fig. 6.4. Frequency dependences of the group velocity of normal waves in a pipeline

The spreading of the acoustic emission signal in time caused by the group velocity dispersion, which significantly worsens the accuracy of determining the arrival time and, as a result, the coordinates of AE sources, has led to the creation of various methods for additional processing of signal waveforms. In [7], the following method was proposed: the signal is passed through a frequency filter, within which the group velocities of each of the modes A_0 and S_0 are practically independent of frequency, but they differ significantly from each other. As a result, it becomes possible to separate two modes in the processed signal, which makes it possible to significantly increase the location accuracy.

However, all these methods use only a small part of the information contained in the waveform of the signal to separate the modes and clarify the time of arrival. A much more powerful method of analysis is the use of time-frequency signal transformations, the most famous and convenient of which are wavelet spectrograms.

6.2. Wavelet transform

Varieties of wavelet analysis, which appeared in the 1980s and significantly enriched the possibilities of signal processing in comparison with the Fourier transform, a large amount of literature is devoted to it. However, in the field of acoustic emission, modifications of this method began to be applied only in 1996 [8].

Wavelet spectrogram (continuous wavelet transform) is a special signal transformation that allows you to show the distribution of signal energy both in time and in frequency. The windowed Fourier transform provides similar opportunities, but it has a lower resolution, a limited frequency range, and a larger number of calculations, compared to wavelets, required to obtain it.

For processing AE impulses, it is convenient to use the well-known formula for continuous wavelet transform

$$W(t, s) = |s|^{-1/2} \int_{-\infty}^{\infty} A(\tau) \psi^* \left[\frac{\tau - t}{s} \right] d\tau$$

replace the scale s with the variable $f=2\pi/s$, which carries information about the frequency of the signal:

$$W(t, f) = \sqrt{|2\pi f|} \int_{-\infty}^{\infty} A(\tau) \psi^* [2\pi f \cdot (\tau - t)] d\tau$$

In this article, the Morlet wavelet is used as the mother wavelet:

$$\psi(x) = \exp(ix - x^2 / 2)$$

The dependence of the modulus of the value $W(t, f)$ on the variables t and f makes it possible to judge the distribution of the signal energy density over time and frequency, respectively. Since $|W(t, f)|$ is a real function of two variables, its graph would be a curved surface. Therefore, to visualize spectrograms, it is more convenient to use a color graph, the abscissa axis on which corresponds to time, the ordinate axis to frequency, and the energy density distribution is displayed using different shades of color (in this article, purple and blue shades correspond to the minimum density, red and yellow to the maximum). In Fig. 6.5, for explanation, a signal is shown, which is a sinusoid with a constant amplitude and a variable frequency, and its wavelet spectrogram. As can be seen from Fig. 6.5, the frequencies corresponding to the maxima in the spectrogram are equal to the frequencies of the original signal.

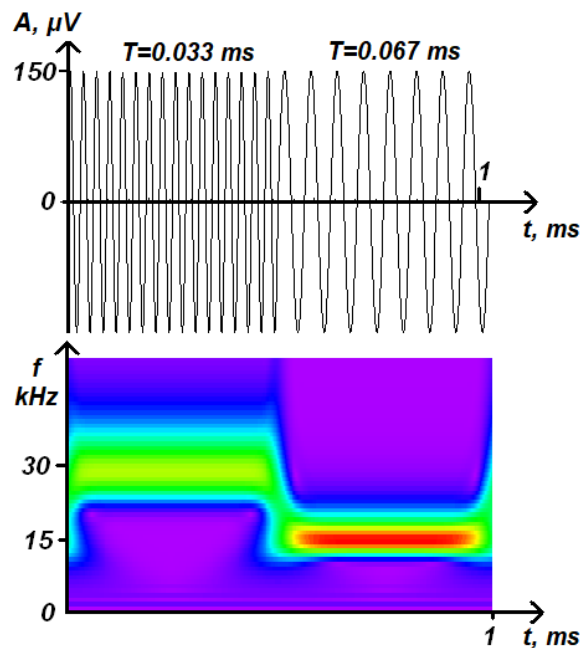


Fig. 6.5. Variable sine wave

From a graph with dispersion curves, you can get a graph of the arrival times of various frequency components of the signal at the AE sensor, located at a distance L from the source. To do this, it is enough to swap the velocity and frequency axes, and then convert the velocity axis v into the time axis t according to the formula $t=L/v+t_0$ (Fig. 6.6), where t_0 is the moment of signal emission. Since the new coordinate axes coincide with the axes on the spectrogram, the resulting graph can be superimposed on the wavelet transform of the signal. In Fig. 6.6, the signal obtained by numerical simulation of the AE from the source that emitted at time t_0 is used and located at the same distance L from the AE sensor. The comparison shows that the energy density maxima in the spectrogram coincide with the dispersion curves. This result justifies the use of the following technique [9] for determining the distance to an AE source from a single waveform: a wavelet spectrogram of the signal is constructed, dispersion curves for the testing object are calculated, then such values of L and t_0 , at which the transformed dispersion curves coincide with the characteristic maxima of the energy distribution on the spectrogram. As a rule, on the wavelet spectrogram, it is convenient to focus on the characteristic frequency mentioned above, at which the values of the group velocities of the modes A_0 , S_0 and A_1 . The location accuracy can be reduced in case of strong noise, with a small distance between the source and the AE sensor, or in the presence of a large number of modes in the signal [10].

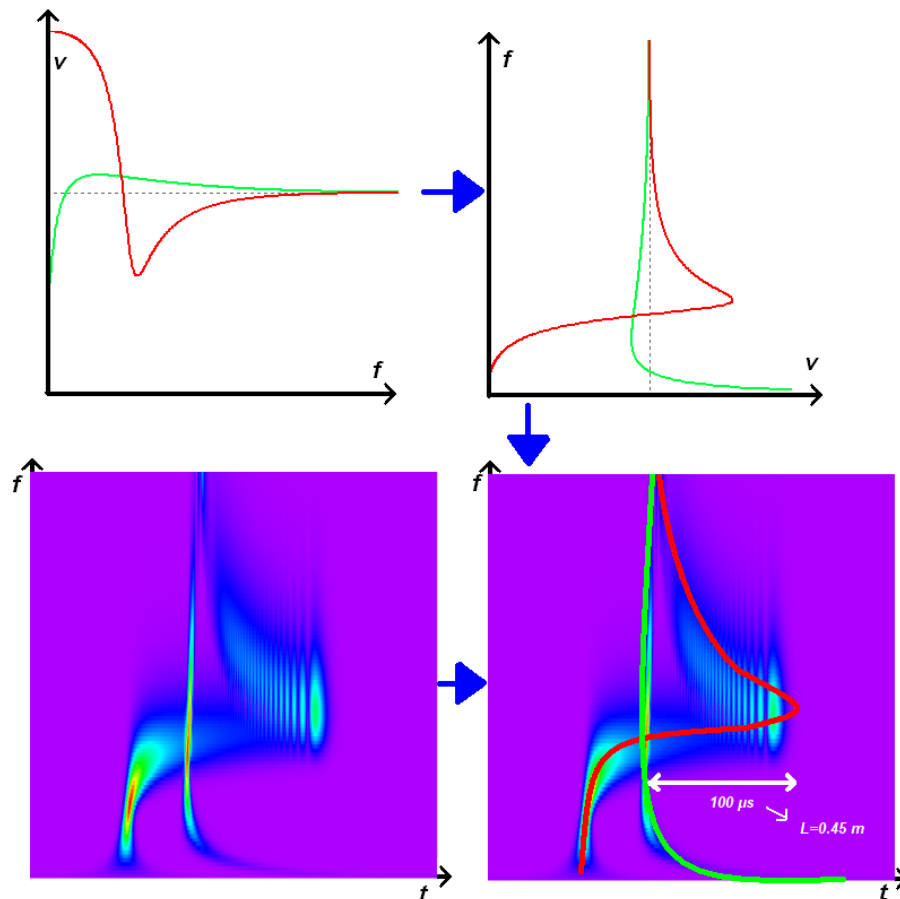


Fig. 6.6. Overlapping dispersion curves and determining the distance to the source

While the main energy of the signal is concentrated along the lines of the dispersion curves, the energy of the noise, which has a wide spectrum and is not localized in time, is evenly distributed over the entire spectrogram (Fig. 6.7). Thus, due to the transition from a one-dimensional dependence to a two-dimensional one, the use of the wavelet transform makes it possible to increase the signal-to-noise ratio [11].

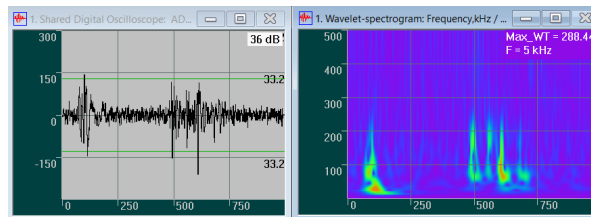


Fig. 6.7. Signal out of the noise

When superposition of dispersion curves is not feasible, you can use the wavelet transform to refine the time of arrival by determining the maximum energy density on the spectrogram or determining the maximum energy density on the spectrogram at a pre-selected frequency. The moment of time corresponding to this maximum can be used to locate the AE source instead of the commonly used threshold crossing time or the time of the signal amplitude maximum [11-12]. Using the value of the guided wave velocity at the frequency corresponding to the maximum makes it possible to reduce the error in determining the coordinates of the AE source.

Because phase information is removed in the type of wavelet transform used here, the reflections in the spectrogram become more similar to the original signal and to each other than in the original waveform (Fig. 6.8), which gives additional options for filtering them. In addition, the spectrogram easily distinguishes interferences with a constant frequency, which in this representation look like horizontal stripes (Fig. 6.9).

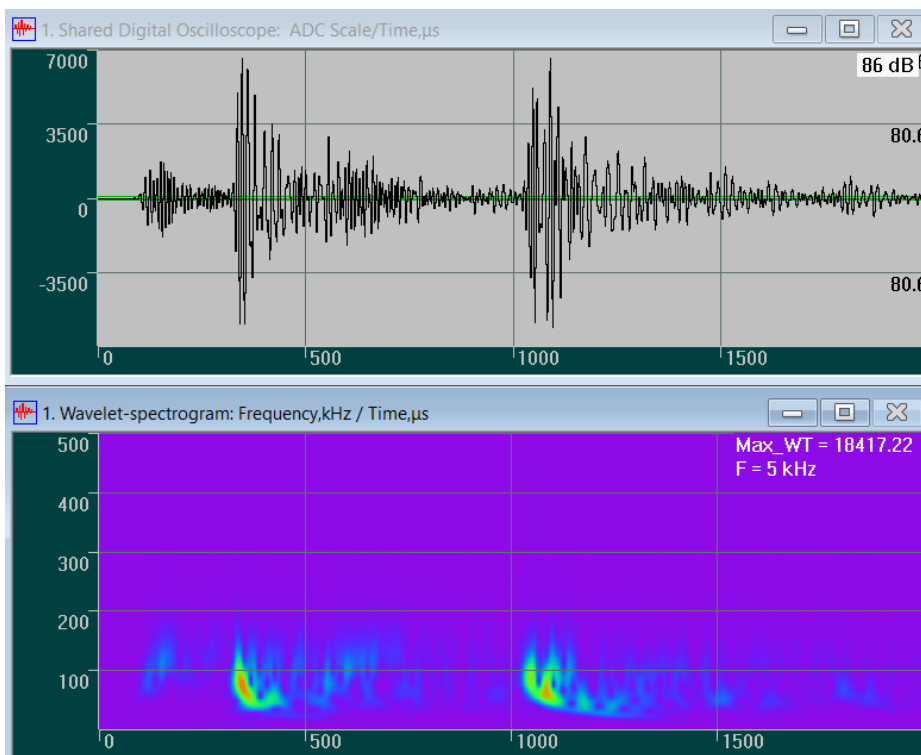


Fig. 6.8. Reflections

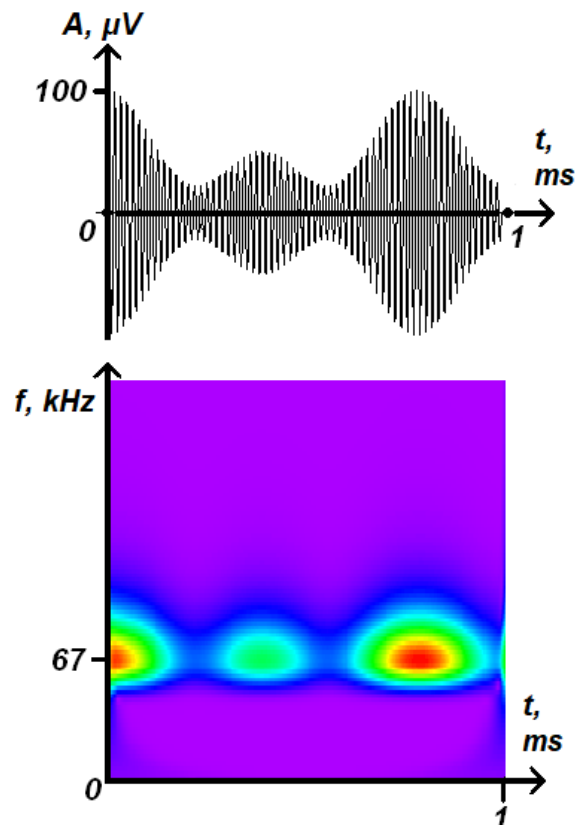


Fig. 6.9. Interferences

Thus, wavelet analysis of AE impulses improves noise filtering, separates acoustic modes, and also provides an alternative way to determine source coordinates. Methods for calculating and visualizing the frequency dependences of group velocities and wavelet spectrograms of AE impulses were built into the A-Line OSC software, and an intuitive interface was implemented for determining the distance L to the AE source by superimposing dispersion curves on the wavelet spectrogram of the signal.

6.3. Little help for beginners

In the **A-Line OSC** program, the main menu item **View – Dispersion curves** makes available the dialog for plotting the frequency dependence of the group velocity of Lamb waves (dispersion curves) in the testing object.

Before plotting curves, you must specify the acoustic properties of the material. To do this, make the necessary choice in the list of materials or assign suitable values in the corresponding fields of the velocities of the longitudinal and transverse waves. If necessary, specify the acoustic properties of the liquid filling the testing object. To do this, select the desired option in the corresponding list or set the required value for the velocity of the longitudinal wave in the liquid.

Next, specify the value of the wall thickness of the testing object in mm (for example, 14.5).

Click the **Recalculate** button to calculate and build a new graph in the graphics field of the dialog. The X axis on the graph shows the frequency in kHz, and the Y axis shows the group velocity in m/s. In the **Curves paint settings** it is possible to enable / disable the displaying of

various modes on the graphs and change their color. By default, it is recommended to output the zero-order antisymmetric mode A_0 and the zero-order symmetric mode S_0 , which usually account for the largest part of the energy of the acoustic signal.

The **Wavelet spectrogram** window is recalculated and drawn when switching to a new waveform. In the case when the visualization of the wavelet spectrogram significantly slows down the scrolling of frames with waveforms, it is recommended to deselect the switch to the left of the inscription **SG** in the **view bar**.

To the right of the **WT** item, you can adjust the color scheme by changing the **Colorfactor** parameter, which is 1 by default. Increasing the value of this parameter improves the visibility of weak components on the signal spectrogram.

To superimpose dispersion curves on the spectrogram, make a choice on the **Group velocities** switch of the **View bar**. Switching on / off the overlay of various modes and changing their color is available from the main menu **View – Dispersion curves** in the paragraph **Curves paint settings** described above.

Use the sliders (two white vertical and one white horizontal lines) to change the overlay parameters of the dispersion curves in such a way that the curves match the maximums on the wavelet spectrogram in the best possible way. The left slider corresponds to the arrival of the fastest Lamb wave (S_0 at $f \rightarrow 0$), the right slider corresponds to the arrival of high-frequency components (all modes at $f \rightarrow \infty$). The horizontal slider allows you to refine the value of the wall thickness in case it is not known in advance.

In the upper right corner of the window with the spectrogram, the signal emission time t_0 (relative to the start time of the waveform), the distance to the source L and the wall thickness d corresponding to the selected overlay are displayed dispersion curves.

For large values of the distance to the source, when the fastest Lamb wave arrives before the start time of the waveform, use the right mouse button to call the context menu, the **X Scale** item and enter a negative time value in the **Range / From** field.

The program saves the position of the sliders for each channel as it runs. When you exit the program, a dialog will be displayed asking you to save the set parameters for superimposing dispersion curves. Click the **Yes** button to save these values until the next session with the program.

To change the maximum frequency displayed on the spectrogram (500 kHz by default), call the **Adjusting the main parameters** dialog from the main menu item **Window – Parameters**, where in the **Max frequency** frame set the maximum frequency, as well as the used for visualization frequency resolution (default 10 kHz). Assigning a smaller value to the frequency resolution leads to a large amount of computer time for calculating the wavelet transform.

6.4. References

1. Pochhammer L. Ueber die Fortpflanzungsgeschwindigkeiten Schwingungen in einem unbegrenzten isotropen Kreiscylinder // J. reine und angew. Math. – 1876. – 81, №4. - S. 324-336.
2. Chree C. Longitudinal vibrations of a circular bar // Quart. J. Pure and Appl. Math. // 1886. – 21, №83/84. – P. 287-298.
3. Gazis D. C. Three-Dimension of the Propagation of waves in Hollow Circular Cylinders. // J. Acoust. Soc. Amer. – 1959. – 31, №3. – P. 568-578.
4. PCdisp - Propagation of Ultrasound in Cylindrical Waveguides.

<http://www.iai.csic.es/users/fseco/pcdisp/pcdisp.htm>

5. Seco F., Martin J.M., Jimenez A., Pons J.L., Calderon L., Ceres R. PCdisp: a tool for the simulation of wave propagation in cylindrical waveguides. // 9th International Congress on Sound and Vibration, in Orlando, Florida (2002). <http://www.iai.csic.es/users/fseco/papers/orlando02.pdf>

6. Auld B.A. Acoustic fields and waves in solids. Volume II. A Wiley-Interscience publication. New York. 1973.

7. Pullin R., Theobald P., Holford K.M., Evans S.L. Experimental Validation of Dispersion Curves in Plates for Acoustic Emission. // Proceedings of the 27thth European Conference on Acoustic Emission Testing (EWGAE 2006), Cardiff, Wavel, UK. PP. 53-60.

8. Suzuki H., Kinjo T., Hayashi Y., Takemoto M., Ono K., Appendix by Hayashi Y., "Wavelet Transform of Acoustic Emission Signals", Journal of Acoustic Emission, Vol. 14, No.2 (1996, April-June), pp. 69-84.

9. Hamstad, M. A., A. O’Gallagher and J. Gary, "Examination of the Application of a Wavelet Transform to Acoustic Emission Signals: Part 2. Source Location", Journal of Acoustic Emission, 20, 2002, 62-81.

10. Cole P., Miller S. Use of advanced A.E. analysis for source discrimination using captured waveforms. 3rd MENDT - Middle East Nondestructive Testing Conference and Exhibition - 27-30 Nov 2005 Bahrain, Manama. <http://www.ndt.net/article/mendt2005/pdf/30.pdf>

11. Hamstad M. A., O’Gallagher A. Effects of noise on lamb-mode acoustic-emission arrival times determined by wavelet transform. Journal of Acoustic Emission, 23, 2005, 1-24.

12. Hamstad, M. A., A. O’Gallagher and J. Gary, "Examination of the Application of a Wavelet Transform to Acoustic Emission Signals: Part 1. Source Identification", Journal of Acoustic Emission, 20, 2002, 39-61.

13. PACshare WaveletsPlus Software.

14. AGU-Vallen Wavelet. <http://www.vallen.de/wavelet/index.html>

15. Kinjo T., Suzuki H., Saito N., Takemoto M., Ono K. Fracture-Mode Classification Using Wavelet-Transformed AE Signals from a Composite. Journal of Acoustic Emission, 15, 1997, 19-32.

16. Takuma M., Shinke N., Ono K. Wavelet Transform Of Magnetomechanical Acoustic Emission Under Elastic Tensile Stress With Displacement Sensor. Journal of Acoustic Emission, 16, 1998, S134-S141

17. Downs, K. S., Hamstad, M. A., A. O’Gallagher, "Wavelet Transform Signal Processing to Distinguish Different Acoustic Emission Sources," Journal of Acoustic Emission, 21, 2003, 52-69.

18. Hamstad, M. A., K. S. Downs A. O’Gallagher "Practical Aspects of Acoustic Emission Source Location by a Wavelet Transform" , Journal of Acoustic Emission, 21, 2003, 70-94, A1-A7.

19. Bayray M., Rauscher F. Wavelet transform analysis of experimental AE wave-forms on steel pressure vessel. Journal of Acoustic Emission, 24, 2006, 22-43.

20. Takuma M., Shinke N., Nishiura T., Akamatu K. Acoustic emission evaluation systems of tool life for shearing of piano and stainless steel wires. Journal of Acoustic Emission, 24, 2006, 52-66.

21. Hamstad M. A. Small diameter waveguide for wideband acoustic emission. *Journal of Acoustic Emission*, 24, 2006, 234-247.



Chapter 7. Manufacturer information

Manufacturer: INTERUNIS-IT LLC.

Address: 111024, Moscow, shosse Entuziastov, 20B, POB 140.

Tel/Fax: +7 (495) 361-76-73, +7 (495) 361-19-90.

E-mail: info@interunis-it.ru

Website: www.interunis-it.ru

